

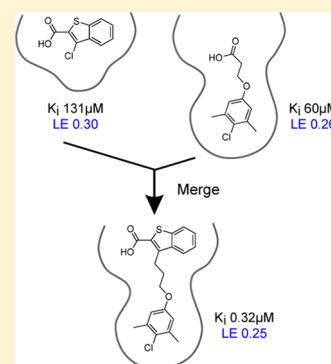
# Discovery of Potent Myeloid Cell Leukemia 1 (Mcl-1) Inhibitors Using Fragment-Based Methods and Structure-Based Design

Anders Friberg, Dominico Vigil, Bin Zhao, R. Nathan Daniels, Jason P. Burke, Pedro M. Garcia-Barrantes, DeMarco Camper, Brian A. Chauder, Taekyu Lee, Edward T. Olejniczak, and Stephen W. Fesik\*

Department of Biochemistry, Vanderbilt University School of Medicine, 2215 Garland Avenue, 607 Light Hall, Nashville, Tennessee 37232-0146, United States

**S** Supporting Information

**ABSTRACT:** Myeloid cell leukemia 1 (Mcl-1), a member of the Bcl-2 family of proteins, is overexpressed and amplified in various cancers and promotes the aberrant survival of tumor cells that otherwise would undergo apoptosis. Here we describe the discovery of potent and selective Mcl-1 inhibitors using fragment-based methods and structure-based design. NMR-based screening of a large fragment library identified two chemically distinct hit series that bind to different sites on Mcl-1. Members of the two fragment classes were merged together to produce lead compounds that bind to Mcl-1 with a dissociation constant of <100 nM with selectivity for Mcl-1 over Bcl-xL and Bcl-2. Structures of merged compounds when complexed to Mcl-1 were obtained by X-ray crystallography and provide detailed information about the molecular recognition of small-molecule ligands binding Mcl-1. The compounds represent starting points for the discovery of clinically useful Mcl-1 inhibitors for the treatment of a wide variety of cancers.



## INTRODUCTION

Mcl-1 (myeloid cell leukemia 1) is a member of the Bcl-2 family of proteins that when dysregulated prevents cancer cells from undergoing programmed cell death, a hallmark of cancer.<sup>1</sup> By overexpression of the Mcl-1 protein or amplification of the Mcl-1 gene, a cancerous cell can avoid death, the normal fate for cells exhibiting abnormal and deregulated growth.<sup>2,3</sup> Indeed, amplification of Mcl-1 is one of the most common genetic aberrations observed in human cancer,<sup>4,5</sup> including lung, breast, prostate, pancreatic, ovarian, and cervical cancers, as well as melanoma and leukemia.<sup>6–13</sup> Moreover, Mcl-1 overexpression has emerged as a resistance mechanism against a number of anticancer therapies including the widely prescribed microtubule-targeted agents paclitaxel and vincristine<sup>14</sup> as well as gemcitabine,<sup>15</sup> a first-line treatment option for pancreatic cancer. Mcl-1 overexpression also confers resistance to ABT-263, a Bcl-2/Bcl-xL inhibitor currently in clinical trials.<sup>16–18</sup> Not surprisingly, specific down-regulation of Mcl-1 by RNA interference inhibits cell growth and colony formation, induces apoptosis in pancreatic cancer cells in vitro, and markedly decreases tumorigenicity in mouse xenograft models.<sup>15</sup> Silencing of Mcl-1 also potently kills particular subgroups of non-small-cell lung cancer (NSCLC) cell lines.<sup>19</sup> Together, these data suggest that direct inhibition of Mcl-1 could be an effective therapeutic option for a wide variety of cancers. In an attempt to target Mcl-1 for the treatment of cancer, small-molecule inhibitors<sup>20–22</sup> and stapled helix peptides<sup>23,24</sup> that bind to Mcl-1 have been reported. However, no Mcl-1 inhibitors have entered clinical trials. Indeed, targeting Mcl-1 is extremely difficult, since Mcl-1 exerts its activity through protein–protein interactions involving a large binding interface. To overcome the challenges associated with

targeting Mcl-1, we applied a combination of fragment-based methods<sup>25</sup> and structure-based design.<sup>26</sup> A similar approach was successfully utilized in the discovery of ABT-263<sup>27,28</sup> and in the discovery of inhibitors against other challenging protein targets, such as Hsp90<sup>29</sup> and BACE.<sup>30</sup> Fragment-based drug discovery (FBDD) takes advantage of sensitive biophysical methods to detect the binding of molecular fragments (MW < 300 Da) that bind weakly to their target proteins. This approach leads to a more efficient sampling of chemical space and can provide hits with higher ligand efficiencies.<sup>31,32</sup> Furthermore, the affinity of the initial fragment hits can be markedly increased by growing, linking, or scaffold merging to obtain potent lead molecules.

Here, we describe the discovery of potent small-molecule Mcl-1 inhibitors ( $K_i$  < 100 nM) that inhibit BH3-containing peptides from binding to Mcl-1. An NMR-based fragment screen yielded two distinct classes of hits that were shown by NMR to bind to two different regions of Mcl-1. On the basis of NMR-derived structural information, the hits from the two classes were merged together to obtain potent Mcl-1 inhibitors that exhibited >100-fold enhanced binding affinity over each component separately. Improved analogues were rapidly optimized by exploiting the SAR observed for the initial fragment hits. Crystal structures of inhibitor-bound Mcl-1 complexes validate the design strategy and also provide detailed structural information for the discovery of more potent inhibitors.

**Received:** October 5, 2012

**Published:** December 17, 2012

## RESULTS

**Hit Identification.** Recombinant, isotopically labeled Mcl-1 (residues 172–327) was used to screen our curated fragment library (>13 800 compounds) by recording SOFAST  $^1\text{H}$ – $^{15}\text{N}$  HMQC spectra of Mcl-1 (Figure 1) incubated with mixtures of

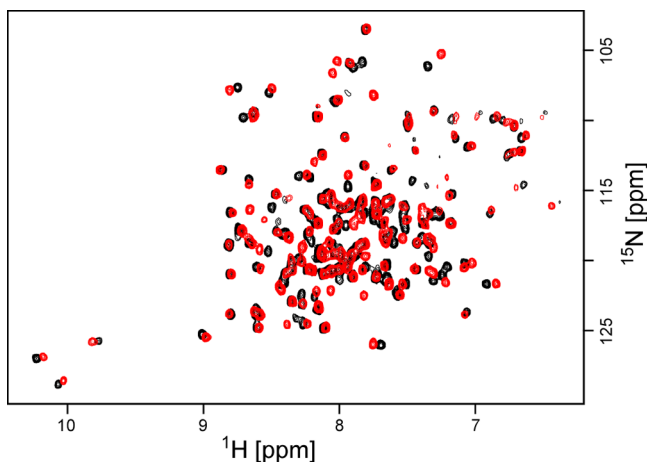


**Figure 1.**  $^1\text{H}$ – $^{15}\text{N}$  HMQC spectra of Mcl-1 with (red) and without (black) fragment 3. The NMR sample contained 50  $\mu\text{M}$   $^{15}\text{N}$ -labeled protein and 800  $\mu\text{M}$  ligand.

12 fragments. Deconvolution of the mixtures by screening individual compounds yielded 132 hits (0.95% hit rate) of 11 distinct chemical classes. Of the initial hits, 93 inhibited Mcl-1 with  $K_i < 500 \mu\text{M}$ , and more than a quarter of the hits demonstrated a ligand efficiency (LE) of 0.25 or greater. Analogues were tested at a single concentration (400  $\mu\text{M}$ ) for their ability to displace a FITC-labeled Mcl-1-derived BH3 peptide from binding to Mcl-1 in a fluorescence polarization anisotropy (FPA) assay.

On the basis of their affinity and distinct chemical characteristics, two classes of compounds were selected for follow-up experiments (Table 1).  $K_i$  values were derived from competition FPA assays measuring the disruption of Mcl-1 and a FITC-Mcl-1-BH3 peptide or of Bcl-xL and Bcl-2 and a FITC-BAK-BH3 peptide. Class I fragment hits contained 6,5-fused heterocyclic carboxylic acids. Analogues of the hits were obtained to explore the SAR. Parent benzothiophene-, benzofuran-, and indole-2-carboxylic acids were not identified in our initial screen because of their weak affinity (1, 6, and 12). The class I fragment hits identified in the screen contained one or two Cl and/or Me substitutions that significantly improved their binding affinities. Similar trends in the SAR for all three core series suggest that they may display similar binding modes. The fragment SAR also suggests that the 3-, 4-, and 6-positions are preferred sites for substitutions and that multiple substitutions can be tolerated or even beneficial in some combinations. For the indole series, a 1-Me substitution exerted similar effects as 3-Cl or 3-Me on benzothiophene and benzofuran scaffolds, suggesting that this core unit could be flipped along its long axis when bound. Interestingly, Mcl-1 inhibitors containing indole acids have also been recently reported in the patent literature.<sup>33,34</sup>

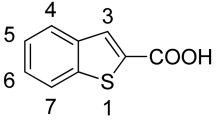
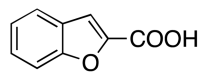
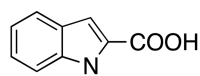
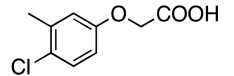
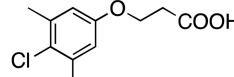
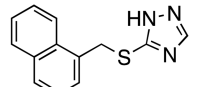
Another structurally distinct group of fragment hits (class II) consists of a hydrophobic aromatic system tethered by a linker to a polar functional group, most often a carboxylic acid (Table 1). Of the hits in this series, 4-chloro-3,5-dimethylphenyl and 1-

naphthyl groups as contained in compounds 17 and 18, respectively, were found to be preferred for binding to Mcl-1.

**NOE-Guided Fragment Docking.** To determine how class I and II fragments bind to Mcl-1, we performed NMR-based structural studies of Mcl-1/fragment hit complexes. Using double-labeled ( $^{15}\text{N}$ ,  $^{13}\text{C}$ ) Mcl-1 protein, we acquired NOE-derived distance restraints and used these to dock representative fragments into a previously determined Mcl-1/Bim BH3 peptide complex (PDB code 3KJ2<sup>35</sup>). Compounds were docked using a simulated annealing protocol in XplorNIH, followed by energy minimization of such models in MOE 2011.10 (Chemical Computing Group Inc.). Fragments representing classes I and II exhibited different patterns of protein/ligand NOEs, confirming that they bind to different regions of Mcl-1. The model structures obtained by this method were consistent with the observed NOEs. A model for Mcl-1 complexed to a compound representative of class I (compound 5) is shown in Figure 2A. Compound 5 displayed NOEs from A227, M231, and F270 to the six-membered ring of the ligand. In this model the acid at the 2-position points toward R263. An NOE-derived model of a fragment hit representing class II (compound 17) is depicted in Figure 2B. In this case, NOEs from M250, F270, and V249 to the two methyl groups of the 4-chloro-3,5-dimethylphenyl indicate that this aromatic group sits deep in the pocket. Additional NOEs from V253 to the aliphatic tether show that the carboxylic acid sits at the surface of the pocket. The NMR-derived models demonstrate that the hydrophobic portions of the two classes of molecules bind to adjacent parts of a large pocket and that the carboxylic acids of both series point toward and likely interact with R263. These results explain the observation that class I and class II compounds are not able to bind simultaneously to Mcl-1.

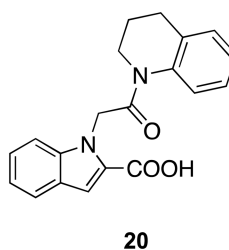
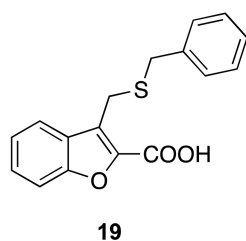
**Fragment Merging and Linker Optimization.** NOE-guided molecular modeling positioned the class I heterocycles above the hydrophobic pocket utilized by the class II compounds. This arrangement suggests that the attachment of class II aromatic groups with a two- to four-atom linker to the 3-position of the class I 6,5-fused heterocycles would lead to merged compounds that maintain the favorable hydrophobic contacts of both fragments to Mcl-1 as well as the interaction between the common carboxylic acid and R263 of Mcl-1. Support for this linking strategy was also obtained from compounds identified and tested from the Vanderbilt Institute of Chemical Biology chemical collection, compounds 19 and 20 (Table 1), that exhibited Mcl-1 binding affinities of 62 and 87  $\mu\text{M}$ , respectively. In order to test this hypothesis, the fragment hits for which we obtained NMR-derived model structures (Figure 2) were linked together. Scaffold merging produced a compound with greater than 2 orders of magnitude improved binding affinity (Figure 3). To determine the optimum linker length, a 1-naphthyl group was connected to the benzothiophene- and benzofuran-2-carboxylic acid cores at the 3-position using two- to four-atom linkers. Table 2 summarizes the Mcl-1 binding affinities for merged compounds with varying linker lengths. The two series of compounds containing different core units showed a parallel SAR, and all merged compounds 21–26 exhibited markedly enhanced binding affinity compared to the unsubstituted cores 1 and 6, confirming the validity of the linking strategy. Although the two- and three-atom linked compounds led to a significant increase in potency, the four-atom linked compounds (e.g., 23 and 26) yielded the most potent Mcl-1 inhibitors in the series, displaying submicromolar dissociation constants. Moreover, these compounds exhibited selectivity for binding to Mcl-1 over Bcl-xL and Bcl-2 (Table 2).

Table 1. SAR of Class I and II Fragment Hits for Binding to Bcl-2 Family Proteins

| Class I   |   |                                      |                                      |        |            |            |
|---|---|--------------------------------------|--------------------------------------|--------|------------|------------|
| structure   | compd   | substitution                         | $K_i$ ( $\mu\text{M}$ ) <sup>a</sup> |        |            | LE (Mcl-1) |
|   |   |                                      | Mcl-1                                | Bcl-xL | Bcl-2      |            |
|  | 1   | H                                    | >1000                                |        |            |            |
|   | 2   | 3-Cl                                 | 131                                  |        |            | 0.30       |
|   | 3   | 3,4-di-Cl                            | 22                                   | >1000  | >1000      | 0.33       |
|   | 4   | 3,6-di-Cl                            | 59                                   |        |            | 0.30       |
|   | 5   | 3-Cl-6-Me                            | 40                                   | 230    | >1000      | 0.31       |
|  | 6   | H                                    | >1000                                |        |            |            |
|   | 7   | 3-Me-5-Cl                            | 52                                   |        |            | 0.31       |
|   | 8   | 3-Me-6-Cl                            | 23                                   |        |            | 0.33       |
|   | 9   | 3,7-di-Me                            | 102                                  | >1000  | >1000      | 0.29       |
|   | 10  | 3,6,7-tri-Me                         | 214                                  | >1000  | >1000      | 0.24       |
|   | 11  | 4-Br- 6-Cl                           | 90                                   |        |            | 0.29       |
|  | 12  | H                                    | >1000                                |        |            |            |
|   | 13  | 1-Me                                 | 160                                  |        |            | 0.29       |
|   | 14  | 1-Me-5-Br                            | 81                                   |        |            | 0.29       |
|   | 15  | 3-Ph-7-Me                            | 136                                  | >1000  | >1000      | 0.20       |
| Class II  |   |                                      |                                      |        |            |            |
| compd   | structure   | $K_i$ ( $\mu\text{M}$ ) <sup>a</sup> |                                      |        | LE (Mcl-1) |            |
|   |   | Mcl-1                                | Bcl-xL                               | Bcl-2  |            |            |
| 16  |   | 103                                  | >1000                                | >1000  | 0.31       |            |
| 17  |  | 60                                   | >1000                                | >1000  | 0.26       |            |
| 18  |  | 86                                   | >1000                                | >1000  | 0.24       |            |

<sup>a</sup>  $K_i$  values are measured in duplicate.

Analogues from the Vanderbilt compound library



**SAR of the Merged Compounds.** To further improve the binding affinity to Mcl-1, the binding contribution of the hydrophobic group of the class II fragments was investigated (Table 3). A library of indoles (**27–48**) tethered by the optimized four-atom linker to various aromatic groups containing different substitution patterns and sizes was prepared. The parent indole **27** with an unsubstituted phenyl group ( $K_i = 35 \mu\text{M}$ ) showed a marginal increase in affinity over the initial fragment hits in the class (**13–15**). Substitutions at the 2'-position (**28, 29**) on the phenyl group yielded only a minor increase in potency. However, potency was remarkably enhanced (20-fold) by monosubstitution of small groups at the 3'-position, as demonstrated by compounds **30** and **31** containing 3'-Me and

3'-CF<sub>3</sub> substitutions, respectively. An increase in affinity was also observed for 4'-Cl substitutions as exemplified by compound **33**. When these beneficial groups were combined, the effect was additive. For example, compound **35** which contains a 3'-Me-4'-Cl-phenyl group displays a 90-fold improved potency over the parent molecule **27**. Indole **37** containing a 3',5'-di-Me-4'-Cl-phenyl also exhibited a similar potency as **35**, whereas increasing the size of the 3'-substitution resulted in a slight reduction in affinity as evidenced by compound **36**.

Bicyclic aromatic groups, such as 1'-naphthyl, 1'-(4'-Cl-naphthyl), and 1'-(5,6,7,8-tetrahydronaphthyl) as exemplified in compounds **42, 44**, and **45**, exhibited submicromolar binding affinities comparable to that of compound **37**. Interestingly,

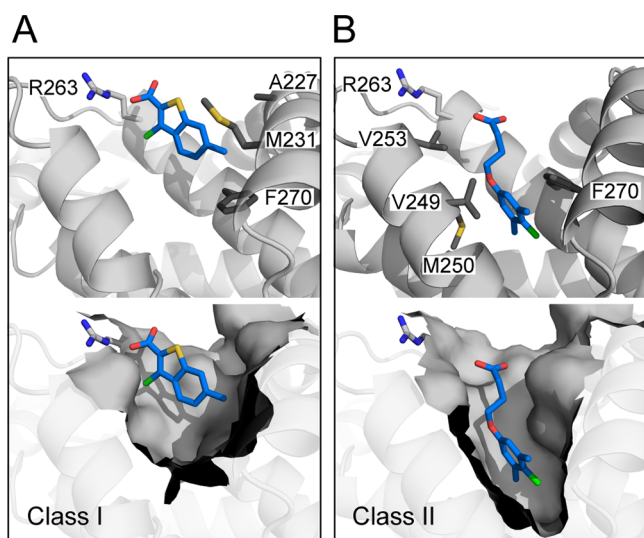


**Figure 2.** Model structures of Mcl-1 complexed to two different classes of fragment hits obtained using NMR-derived distance restraints. Residues (labeled) with NOEs to the fragments (blue) are rendered as sticks (gray). R263 is also labeled. (A) Class I: benzothiophene **5**. (B) Class II: tethered aromatic **17**.

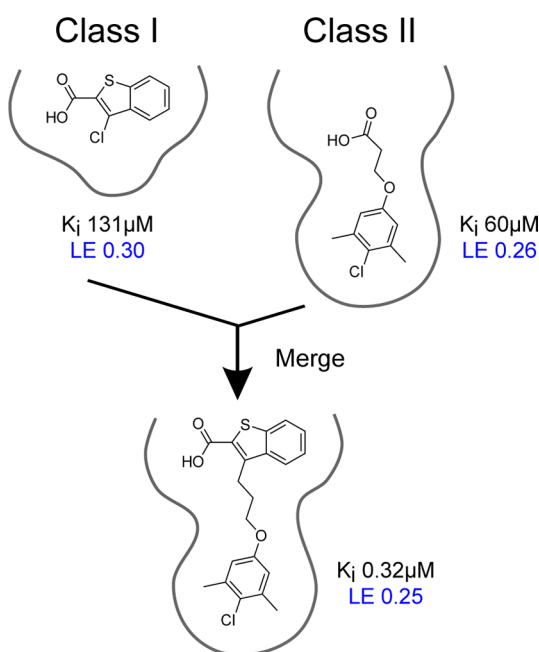


**Figure 3.** Schematic illustrating the merging of fragments **2** and **17** to produce compound **60**. The affinity of each molecule to Mcl-1 is shown as well as the ligand efficiencies.

compound **43** containing a 2'-naphthyl moiety was 20-fold less potent than its regioisomer **42**, indicating that the attachment position to this group is important for optimal binding to Mcl-1. The largest reduction in potency was observed for compounds **47** and **48** with nitrogen-containing heterocycles (6'-quinolinyl and 4'-indole) showing a 190- and 40-fold lower affinity compared to **42**. These observations indicate that binding in the lower part of the pocket is dictated by hydrophobic interactions and that polar moieties are not accommodated in the binding pocket of Mcl-1. Additional substitutions of the core indole nitrogen are also tolerated as shown in compounds **56**–**59**. This SAR trend strongly suggests that size, substitution

pattern, and hydrophobicity of the aromatic group are all essential for binding to Mcl-1. Interestingly, most of the optimal groups identified from the data set were identical to the initial class II fragment hits, demonstrating that the preliminary fragment SAR can guide the optimization of the linked compounds.

The initial fragment SAR indicated that substitutions at the 4- or 6-position are beneficial. The same principles were applied to further optimize the potency of the linked compounds. As expected from the SAR of the fragment hits, 6-Cl adducts (**52**–**55**) displayed a potency increase. In contrast, 4-Cl analogues (**49**–**51**) exhibited mixed results, suggesting that the anchoring unit might cause a subtle alteration in the binding conformation of the core unit. Merged compounds comprising benzothiophene and benzofuran scaffolds revealed similar SAR patterns as the indole series.

An additional linking strategy was explored by attaching compounds to the 1-position of the indole core (Table 4). Compounds **69**–**71** containing the optimized linker and anchor units retained comparable potency as the corresponding 3-substituted indoles. This demonstrates that the core indole can bind in a conformation flipped along its long axis as previously predicted from the SAR of the fragment hits. Finally, the importance of the 2-carboxylic acid was evaluated by converting **71** to an amide as in compound **72**. This single modification resulted in a dramatic reduction in potency of at least 3 orders of magnitude. In line with previous results, merged compounds showed selectivity over Bcl-2 and Bcl-xL, respectively. Compound **53**, for example, is one of the most potent inhibitors of Mcl-1 ( $K_i = 55$  nM, Supporting Information, Figure S1) and displays a 16-fold selectivity over Bcl-2 and 270-fold over Bcl-xL.

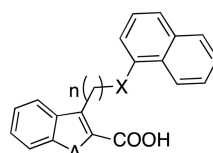
These results clearly demonstrate the effectiveness of fragment-based methods and a structure-guided fragment merging strategy as a very powerful approach for rapidly obtaining potent binders against target proteins. Additionally, the ability to translate the lessons learned from the SAR of the fragment hits to our merged compounds aided the optimization of our lead compounds.

#### X-ray Structures of Merged Compounds Complexed to Mcl-1.

The three-dimensional structures of compounds representing different series of merged compounds in complex with Mcl-1 were obtained by X-ray crystallography (Table 5). As shown in Figure 4 for a representative member of both the benzothiophene and the indole series, the merged compounds occupy both pockets identified by NMR. The Mcl-1 inhibitors bind in the BH3 binding groove and explain why our compounds compete with BH3-peptides for binding to Mcl-1. The overall secondary structures of Mcl-1 in the Mcl-1/inhibitor complexes did not change upon binding the small molecules.<sup>23,36</sup> However, ligand binding does result in several important structural changes near the binding pocket (Figure 5A,B). In compound-bound structures, a pronounced bend was observed in helix 4 ( $\alpha 4$ ) which helps accommodate the anchor unit of the ligand in the deep hydrophobic pocket and places the top of  $\alpha 4$  closer to the ligand. In fact, the top of  $\alpha 4$  protrudes slightly into the BH3 binding cleft. This causes the loop connecting helix 4–5 to be pulled toward the ligand and allows changes in the charge–charge interactions of R263 (Figure 5C,D). The guanidinium group of R263 can now interact with the carboxylate moiety of the merged compounds. These changes are not easily anticipated from the inspection of Mcl-1 complexed with a peptide. In peptide-bound structures,  $\alpha 4$  is straight which keeps the BH3 binding cleft and the connecting loop open to better



Table 2. Optimization of Linker Length in the Merged Compounds



| compd | A | n | X               | $K_i$ ( $\mu\text{M}$ ) |                     |                    |
|-------|---|---|-----------------|-------------------------|---------------------|--------------------|
|       |   |   |                 | Mcl-1 <sup>a</sup>      | Bcl-xL <sup>b</sup> | Bcl-2 <sup>b</sup> |
| 21    | S | 1 | CH <sub>2</sub> | 12.5 $\pm$ 5.6          |                     |                    |
| 22    | S | 2 | CH <sub>2</sub> | 9.6 $\pm$ 3.0           |                     |                    |
| 23    | S | 3 | O               | 0.37 $\pm$ 0.03         | 15                  | 9.7                |
| 24    | O | 1 | CH <sub>2</sub> | 9.5 $\pm$ 2.9           |                     |                    |
| 25    | O | 2 | CH <sub>2</sub> | 14.6 $\pm$ 7.1          |                     |                    |
| 26    | O | 3 | O               | 1.0 $\pm$ 0.44          | >15                 | 4.3                |

<sup>a</sup> $K_i$  values are measured in triplicate. <sup>b</sup> $K_i$  values are measured in duplicate.

accommodate the peptide. The side chain of R263 also adopts a different conformation so that it can interact with D218 of the peptide (Figure 5C). It is also evident that the peptide does not utilize the full capacity of the hydrophobic pocket. In the peptide structure, L213 is only occupying the very upper part of this deep pocket (Figure 6A).

In all of the structures obtained thus far, the hydrophobic unit of the class II fragments binds in the lower part of the pocket (Figure 4). Furthermore, all core units derived from class I fragments are positioned in the upper part of the pocket, directing the carboxylic acid toward R263, and forming an interaction with M231, A227, F228, and F270 via the six-membered ring (Figure 4B).

The SAR of our merged compounds can now be rationalized from a more detailed analysis of the X-ray structures. Positions 1 and 7 of the core unit are surface exposed, and as shown, substitutions here have little or no effect on compound binding. In contrast, there is minimal space for any substitution at the 5-position, which is consistent with results of the observed SAR. The results obtained when adding groups at the 4-position could be explained by slight differences in how the hydrophobic group and the linker are positioned. These subtle changes may affect how much room there is at the 4-position or how the entire core unit is positioned in the binding pocket. Insights regarding the improved affinity due to substitutions at the 6-position can be derived from the X-ray structures. The up to 5-fold increase in binding may be explained by the addition of a hydrophobic group, which fits between M231 and A227 in a previously unoccupied pocket (Figure 4B,C). Presumably the chlorine keeps the core unit in a more favorable position so that the carboxylic acid can make a better interaction with R263 (Figure 5D). The latter interaction also explains the requirement of a negatively charged acidic group in our fragment hits as well as the loss of affinity upon amidation of the carboxylic acid (71, 72).

The SAR of the class II hits was also analyzed in terms of the X-ray structures. From the structures, it is evident why hydrophobic groups are preferred over more hydrophilic aromatic ring systems containing a nitrogen atom (compounds 47 and 48). The pocket is lined with numerous nonpolar side chains, namely, M231, L235, L246, V249, M250, L267, F270, V273, L290, and I294. An overlay of compounds 53 and 60 when bound to Mcl-1 shows a precise overlap of the anchoring 3',5'-di-Me-4-Cl-phenyl group (Figure 4A), suggesting that this unit anchors the rest of the ligand in the binding pocket. This binding pocket is present in both Bcl-xL and Bcl-2; however, it is neither as deep nor as large as it is in Mcl-1. Accessing parts of this pocket not present in other members of the Bcl-2 family provides a possible

explanation for the selectivity of our compounds for binding to specific Bcl-2 family proteins.

## SYNTHESIS

Compounds 21–26 and 60–68 were prepared as outlined in Scheme 1. Selective lithiation at the 3-Me position of compounds 80a,b with LDA at  $-10^\circ\text{C}$  followed by nucleophilic substitution with 1-(bromoalkyl)naphthylenes or 1-(2-bromoethoxy)-naphthalene gave compounds 21–26 with varying linker length to the terminal 1-naphthyl group. 3-Methylbenzothiophene-2-carboxylic acid cores 82a–c containing 4-, 6-, or 7-Cl substitutions were synthesized from the corresponding chloro-(2-fluorophenyl)ethanones (81a–c) by reacting with methyl thioglycolate under DBU followed by saponification of the produced esters. Compounds 82a–c and 80a were then subjected to the alkylation condition described above to yield compounds 60–66. Unlike unsubstituted benzothiophene 80a, it is necessary to employ alkyl iodides as substrates to increase yields because of reduced nucleophilicity of cores 82a–c by the substituted chloride. 5-Cl-Benzofuran 84 was prepared from 83 by reacting with methyl bromoacetate. By use of similar conditions, compounds 67 and 68 were obtained.

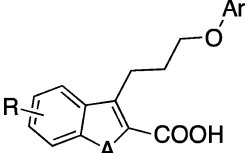
Mcl-1 inhibitors containing indole core 27–59 were synthesized by the route shown in Scheme 2. Indoles 85a–c were prepared utilizing the modified Japp–Klingemann reaction.<sup>37</sup> Selective reduction using excess  $\text{BH}_3$  gave the corresponding alcohols which were then treated with a variety of aromatic alcohols under Mitsunobu conditions to afford the corresponding ether 86. The ether was then saponified to give indoles 27–55. N-Substituted indoles 56–59 were produced through alkylations of selected esters 86 followed by hydrolysis.

Class II fragments, binding in the deep hydrophobic pocket, can also be linked to the indole nitrogen as depicted in Scheme 3. Ethyl indole-2-carboxylate 88 was substituted at the 1-position with ethyl 3-bromopropionate using  $\text{K}_2\text{CO}_3$  as a base under reflux in good yield. The adduct 89 then underwent the same series of reactions to give compounds 69–71. Compound 71 was further functionalized by amidation to produce 72.

## DISCUSSION

Mcl-1 is one of the most frequently amplified genes in human cancers and a common resistance factor to treatment with current chemotherapeutic agents and existing Bcl-2 family inhibitors (e.g., ABT-263 and ABT-199).<sup>4,38</sup> Here, we describe the discovery of small molecules that potently inhibit Mcl-1 using fragment-based methods and structure-based design. The X-ray structures of our merged compounds complexed with Mcl-1

Table 3. SAR of Merged Compounds Containing an Optimized Four-Atom Linker



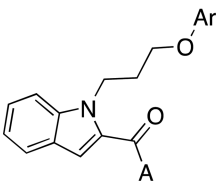
| compd | A   | R    | Ar                             | $K_i$ ( $\mu$ M)   |                     |                    |
|-------|-----|------|--------------------------------|--------------------|---------------------|--------------------|
|       |     |      |                                | Mcl-1 <sup>a</sup> | Bcl-xL <sup>b</sup> | Bcl-2 <sup>b</sup> |
| 27    | NH  | H    | Ph                             | 35 $\pm$ 7.1       |                     |                    |
| 28    | NH  | H    | 2-Me-phenyl                    | 15 $\pm$ 0.7       |                     |                    |
| 29    | NH  | H    | 2-CF <sub>3</sub> -phenyl      | 8.8 $\pm$ 1.7      |                     |                    |
| 30    | NH  | H    | 3-Me-phenyl                    | 1.9 $\pm$ 0.6      |                     |                    |
| 31    | NH  | H    | 3-CF <sub>3</sub> -phenyl      | 1.7 $\pm$ 0.08     |                     |                    |
| 32    | NH  | H    | 4-Me-phenyl                    | 16 $\pm$ 3.1       |                     |                    |
| 33    | NH  | H    | 4-Cl-phenyl                    | 9.8 $\pm$ 2.9      |                     |                    |
| 34    | NH  | H    | 4-CF <sub>3</sub> -phenyl      | 9.9 $\pm$ 3.2      |                     |                    |
| 35    | NH  | H    | 3-Me-4-Cl-phenyl               | 0.38 $\pm$ 0.14    | >15                 | 9.1                |
| 36    | NH  | H    | 3-Et-4-Cl-phenyl               | 1.1 $\pm$ 0.1      |                     |                    |
| 37    | NH  | H    | 3,5-di-Me-4-Cl-phenyl          | 0.30 $\pm$ 0.15    | >15                 | 5.3                |
| 38    | NH  | H    | 3-(1,1'-biphenyl)              | 7.7 $\pm$ 2.1      |                     |                    |
| 39    | NH  | H    | 4-(1,1'-biphenyl)              | 7.6 $\pm$ 0.7      |                     |                    |
| 40    | NH  | H    | 3-phenoxyphenyl                | 5.2 $\pm$ 0.3      |                     |                    |
| 41    | NH  | H    | 4-phenoxyphenyl                | 6.4 $\pm$ 0.6      |                     |                    |
| 42    | NH  | H    | 1-naphthyl                     | 0.33 $\pm$ 0.10    | >15                 | 2.7                |
| 43    | NH  | H    | 2-naphthyl                     | 7.5 $\pm$ 0.6      |                     |                    |
| 44    | NH  | H    | 1-(4-Cl-naphthyl)              | 0.48 $\pm$ 0.01    |                     |                    |
| 45    | NH  | H    | 1-(5,6,7,8-tetrahydronaphthyl) | 0.30 $\pm$ 0.10    |                     |                    |
| 46    | NH  | H    | 5-(2,3-dihydroindeny)          | 2.9 $\pm$ 0.1      |                     |                    |
| 47    | NH  | H    | 6-quinolinyl                   | 62 $\pm$ 17        |                     |                    |
| 48    | NH  | H    | 4-indolyl                      | 14 $\pm$ 0.3       |                     |                    |
| 49    | NH  | 4-Cl | 3-Me-4-Cl-phenyl               | 0.81 $\pm$ 0.16    |                     |                    |
| 50    | NH  | 4-Cl | 3,5-di-Me-4-Cl-phenyl          | 0.16 $\pm$ 0.04    |                     |                    |
| 51    | NH  | 4-Cl | 1-naphthyl                     | 0.70 $\pm$ 0.24    |                     |                    |
| 52    | NH  | 6-Cl | 3-Me-4-Cl-phenyl               | 0.19 $\pm$ 0.02    | >15                 | 1.4                |
| 53    | NH  | 6-Cl | 3,5-di-Me-4-Cl-phenyl          | 0.055 $\pm$ 0.018  | >15                 | 0.87               |
| 54    | NH  | 6-Cl | 1-naphthyl                     | 0.075 $\pm$ 0.025  | 6.8                 | 0.96               |
| 55    | NH  | 6-Cl | 1-(5,6,7,8-tetrahydronaphthyl) | 0.066 $\pm$ 0.028  |                     |                    |
| 56    | NMe | H    | 3,5-di-Me-4-Cl-phenyl          | 0.18 $\pm$ 0.01    | >15                 | 7.4                |
| 57    | NMe | H    | 1-naphthyl                     | 0.26 $\pm$ 0.04    | >15                 | >15                |
| 58    | NMe | 6-Cl | 3,5-di-Me-4-Cl-phenyl          | 0.14 $\pm$ 0.01    |                     |                    |
| 59    | NBn | H    | 1-naphthyl                     | 0.29 $\pm$ 0.17    | >15                 | >15                |
| 60    | S   | H    | 3,5-di-Me-4-Cl-phenyl          | 0.32 $\pm$ 0.01    | >15                 | 5.3                |
| 23    | S   | H    | 1-naphthyl                     | 0.37 $\pm$ 0.07    | 15                  | 9.7                |
| 61    | S   | 4-Cl | 3,5-di-Me-4-Cl-phenyl          | 1.3 $\pm$ 0.52     |                     |                    |
| 62    | S   | 4-Cl | 1-naphthyl                     | 1.6 $\pm$ 0.41     |                     |                    |
| 63    | S   | 6-Cl | 3,5-di-Me-4-Cl-phenyl          | 0.25 $\pm$ 0.04    | 4.1                 | 0.80               |
| 64    | S   | 6-Cl | 1-naphthyl                     | 0.12 $\pm$ 0.03    | 6.8                 | 0.96               |
| 65    | S   | 7-Cl | 3,5-di-Me-4-Cl-phenyl          | 0.75 $\pm$ 0.24    |                     |                    |
| 66    | S   | 7-Cl | 1-naphthyl                     | 0.72 $\pm$ 0.15    |                     |                    |
| 67    | O   | H    | 3,5-di-Me-4-Cl-phenyl          | 3.0 $\pm$ 0.10     |                     |                    |
| 26    | O   | H    | 1-naphthyl                     | 1.0 $\pm$ 0.44     | >15                 | 4.3                |
| 68    | O   | 5-Cl | 1-naphthyl                     | 2.5 $\pm$ 1.1      |                     |                    |

<sup>a</sup> $K_i$  values are measured in triplicate. <sup>b</sup> $K_i$  values are measured in duplicate.

identify several opportunities to significantly improve the affinity of the current lead molecules.

Although current lead compounds are able to compete with BH3-containing peptides for binding to Mcl-1, crystal structures reveal that the compounds may not be maximally exploiting the available binding opportunities. For example, pockets occupied by the peptide residues V216, D218, and V220 are currently not

occupied by the compounds (Figure 6). Mutation of V216, D218, and V220 to alanine reduces peptide binding affinity 50-, 5-, and 45-fold, respectively, demonstrating the importance of these additional binding pockets.<sup>23</sup> Expanding our lead compounds to fill more of the peptide interface could yield more potent Mcl-1 inhibitors. In support of this hypothesis is a comparison of one of our current lead molecules bound to Mcl-1

Table 4. SAR of 2-Carboxylate Analogues on 1-Substituted Indoles<sup>a</sup>


| compd     | A               | Ar                    | Mcl-1 $K_i$ ( $\mu$ M) <sup>a</sup> |
|-----------|-----------------|-----------------------|-------------------------------------|
| <b>69</b> | OH              | 3-Me-4-Cl-phenyl      | $1.2 \pm 0.43$                      |
| <b>70</b> | OH              | 3,5-di-Me-4-Cl-phenyl | $0.41 \pm 0.07$                     |
| <b>71</b> | OH              | 1-naphthyl            | $0.47 \pm 0.08$                     |
| <b>72</b> | NH <sub>2</sub> | 1-naphthyl            | >500                                |

<sup>a</sup>The asterisk (\*) indicates that all  $K_i$  values are measured in triplicate.Table 5. X-ray Data Collection and Refinement Statistics<sup>a</sup>

| parameter                           | ligand                 |                        |                             |
|-------------------------------------|------------------------|------------------------|-----------------------------|
|                                     | 53                     | 60                     | 16-mer peptide <sup>b</sup> |
| PDB code                            | 4HW2                   | 4HW3                   | 4HW4                        |
| no. chains                          | 6                      | 12                     | 2                           |
| protein construct                   | Mcl-1 $\Delta$ 5       | Mcl-1 $\Delta$ 5       | Mcl-1 WT                    |
| Data collection                     |                        |                        |                             |
| space group                         | $P2_12_12$             | $P2_1$                 | $P2_1$                      |
| cell dimensions                     |                        |                        |                             |
| <i>a</i> , <i>b</i> , <i>c</i> (Å)  | 121.99, 134.32, 62.04  | 139.44, 58.76, 140.67  | 50.07, 48.35, 68.18         |
| $\alpha$ , $\beta$ , $\gamma$ (deg) | 90.00, 90.00, 90.00    | 90.00, 90.71, 90.00    | 90.00, 93.83, 90.00         |
| resolution (Å)                      | 50.00–2.80 (2.85–2.80) | 50.00–2.40 (2.44–2.40) | 50.00–1.53 (1.56–1.53)      |
| $R_{\text{sym}}$                    | 5.7 (29.7)             | 5.3 (29.9)             | 4.7 (40.8)                  |
| $R_{\text{merge}}$                  | 4.5 (41.1)             | 4.5 (36.4)             | 4.2 (31.3)                  |
| $I/\sigma(I)$                       | 5.7 (1.9)              | 12.5 (4.9)             | 25.0 (2.5)                  |
| completeness (%)                    | 97.7 (95.0)            | 98.2 (96.3)            | 100 (100)                   |
| redundancy                          | 4.1 (3.4)              | 3.5 (2.7)              | 4.1 (3.4)                   |
| Structure Refinement                |                        |                        |                             |
| no. reflections                     | 25 097                 | 88 346                 | 49 292                      |
| $R_{\text{work}}/R_{\text{free}}$   | 21.69/24.52            | 21.51/26.28            | 13.74/18.40                 |
| no. atoms                           |                        |                        |                             |
| protein                             | 7181                   | 14 259                 | 4823 <sup>c</sup>           |
| ligand                              | 190                    | 300                    | 520                         |
| water                               |                        | 252                    | 387                         |
| Ramachandran <sup>d</sup>           |                        |                        |                             |
| preferred regions (%)               | 90.1                   | 89.9                   | 94.5                        |
| allowed regions (%)                 | 7.4                    | 8.4                    | 5.1                         |
| generously allowed (%)              | 1.5                    | 1.2                    | 0.3                         |
| disallowed region (%)               | 1.0                    | 0.6                    | 0.0                         |
| rms deviations                      |                        |                        |                             |
| bond length (Å)                     | 0.026                  | 0.010                  | 0.008                       |
| bond angle (deg)                    | 1.993                  | 1.411                  | 1.005                       |

<sup>a</sup>Values in parentheses represent results for the highest resolution shell. <sup>b</sup>16-mer Mcl-1 BH3-peptide: Ac-ALETLLRRVGDGVQRNH-NH<sub>2</sub>.<sup>c</sup>Including hydrogen atoms. <sup>d</sup>Backbone conformation was analyzed with PROCHECK.<sup>52</sup>

with ABT-737 complexed to Bcl-xL (Figure 6B). Our lead compounds are much smaller than ABT-737 and only use a fraction of the binding pockets.

To identify small molecules that bind to these additional pockets, fragment-based screens of Mcl-1 in the presence of one of our nanomolar leads represent a possible strategy for improving potency. By blocking the initial site, fragments could be identified that bind to these additional pockets of the protein. These fragments could be rapidly incorporated into new molecules to markedly improve binding affinity.

An important lesson learned from these studies is that the SAR observed with the fragment hits is mirrored in the merged compounds and quickly led to the design and synthesis of potent lead molecules. In addition, the selectivity profile of the fragment hits for binding to Bcl-2 family members is mimicked by the merged compounds. The affinity of initial Mcl-1 fragment hits

against the closely related family members Bcl-xL and Bcl-2 revealed a 5- to 50-fold selectivity for binding to Mcl-1 which is retained in the lead compounds.

In summary, this study demonstrates the successful targeting of Mcl-1 by fragment-based and structure-guided methods to quickly produce an initial set of high-affinity and Mcl-1 selective inhibitors. The compounds described here serve as starting points for the discovery of clinically useful Mcl-1 inhibitors for the treatment of cancer.

## EXPERIMENTAL SECTION

**Protein Expression and Purification.** A codon-optimized gene sequence encoding residues 172–327 of human Mcl-1 (Uniprot code Q07820) was purchased (Genscript) and cloned into a Gateway entry vector (pDONR-221, Invitrogen) using the protocols provided (Supporting Information, Table S1). This construct was further subcloned into an expression vector (pDEST-HisMBP) containing a

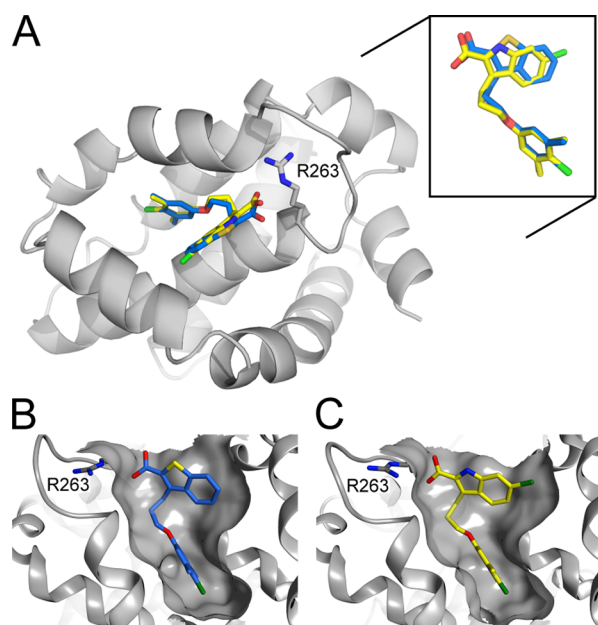


**Figure 4.** X-ray structures of merged compounds bound to Mcl-1. Compounds incorporating different scaffolds (benzothiophene and indole) occupy the same binding pocket and adopt very similar binding poses (inset). (A) Compounds **53** and **60** interact with Mcl-1 in the BH3-peptide binding cleft between helices 3, 4, and 5. Shown is the surface depiction of Mcl-1 when complexed to (B) **60** and (C) **53** that illustrates how the merged compounds fill the pockets as predicted by NMR and interact with R263.

maltose binding protein (MBP) tag for increased solubility, a tobacco etch virus (TEV) protease recognition site for tag removal, and an N-terminal His tag to facilitate purification. The integrity of all plasmids was checked by sequencing. Soluble Mcl-1 protein was expressed in *Escherichia coli* BL21 CodonPlus (DE3) RIL (Stratagene) using ampicillin and chloramphenicol for selection.

In brief, a colony from a fresh transformation plate was picked to inoculate 100 mL of LB medium (37 °C). The overnight culture was used to start a 10 L fermentation (BioFlo 415, New Brunswick Scientific) grown at 37 °C. For NMR studies, uniformly  $^{15}\text{N}$  and  $^{15}\text{N}/^{13}\text{C}$  isotopically labeled protein samples were produced in minimal M9 medium, where  $^{15}\text{NH}_4\text{Cl}$  and  $[\text{U-}^{13}\text{C}]\text{-D-glucose}$  were used as sole nitrogen and carbon sources (Cambridge Isotope Laboratories). When the cell density corresponded to  $\text{OD}_{600} = 2$ , the temperature was lowered to 20 °C. After 1 h, protein expression was induced with 0.5 mM IPTG. Cells were harvested after 16 h by centrifugation. Pellets were frozen and redissolved in lysis buffer (20 mM Tris, pH 7.5, 300 mM NaCl, 20 mM imidazole, 5 mM BME), approximately 100 mL/10 g pellet, before the cells were broken by homogenization (APV-2000, APV). Prior to application to an affinity column (140 mL, ProBond, Invitrogen), lysate was cleared by centrifugation (18 000 rpm) and filtration (0.44  $\mu\text{m}$ ). Bound protein was washed on the column and then eluted by a gradient (20 mM Tris, pH 7.5, 300 mM NaCl, 500 mM imidazole, 5 mM BME). To enhance TEV protease cleavage, samples were buffer exchanged (50 mM Tris, pH 7.5, 100 mM NaCl, 5 mM BME) on three serially connected columns (HiPrep 26/10 Desalting, GE Healthcare). TEV protease was added to a molar ratio of 1:10 (TEV/Mcl-1) and incubated at room temperature until cleavage was complete. After adding 20 mM imidazole to the samples, they were passed over a subtractive second nickel-column (120 mL, Ni-NTA Superflow, Qiagen) to remove the MBP-tag, noncleaved protein, and TEV protease. Mcl-1 protein for NMR screening was buffer exchanged into an optimized NMR buffer (25 mM sodium phosphate, pH 6.3, 25 mM NaCl, 1 mM DTT, 0.01%  $\text{NaN}_3$ ). To achieve highly pure samples (e.g., for crystal screening), a supplementary step of size-exclusion chromatography (HiLoad 26/60, Superdex 75, GE Healthcare) was

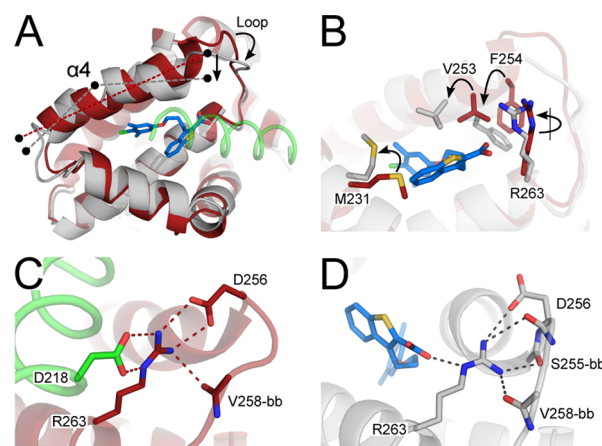


**Figure 5.** Several structural differences between peptide-bound (red) and compound-bound (gray) Mcl-1 complexes were identified. The Mcl-1-derived BH3-peptide is depicted in green and compound **60** in blue. (A) To accommodate the hydrophobic fragments into the deep pocket, helix 4 ( $\alpha 4$ ) is slightly kinked in the structures of Mcl-1/compound complexes compared to the Mcl-1/peptide structures. This leads to further rearrangements of the loop, pulling it toward the merged compound. (B) Close-up of the small-molecule binding site in Mcl-1. Compared to the peptide-bound state, our merged compounds induce changes in the position and/or in rotamer states of nearby residues. (C, D) The network of charge–charge interactions and polar contacts involving R263 are dramatically different in the two types of complexes. (C) While bound to the peptide, R263 of Mcl-1 interacts closely with D218 of the 16-mer, a residue shown to be important by alanine-scanning.<sup>23</sup> Moreover, R263 interacts with the side chain of D256 and the backbone (bb) oxygen of V258 in Mcl-1. (D) When complexed with merged compounds (e.g., **60**), this network is replaced by an interaction to the carboxylic acid of the small-molecule ligand and additional polar contacts to the backbone oxygen atoms of S255 and D256.

implemented. The running buffer also acted as the Mcl-1 storage and crystallography buffer (20 mM HEPES, pH 6.8, 50 mM NaCl, 3 mM DTT, 0.01%  $\text{NaN}_3$ ). Purifications were done at 4 °C, and concentration steps were performed in stirred ultrafiltration cells (Amicon, Millipore).

To improve protein sample quality and to increase crystal diffraction, protein mutants were created by site-directed mutagenesis (Quik-Change, Agilent Technologies). Primers for a C-terminal deletion ( $\Delta 5$ ) were designed using their online tool and ordered from Eurofins MWG Operon. Mutations were made on the entry vector above, analyzed by in-house sequencing, and subsequently transferred into the pDEST-HisMBP expression vector. Mutant proteins were purified in the same way as wild-type (WT) proteins.

**NMR Experiments: Fragment Screening and NOE-Guided Fragment Docking.** Nuclear magnetic resonance (NMR) screening experiments were performed at 30 °C, using either a Bruker Avance III 500 MHz or 600 MHz NMR spectrometer equipped with a 5 mm single-axis z-gradient cryoprobe and a Bruker SampleJet sample changer. Two-dimensional, gradient-enhanced  $^1\text{H}/^{15}\text{N}$  heteronuclear multiple-quantum coherence (SOFAST-HMQC) spectra (32 scans, ~12 min) were used to track shift changes upon ligand binding.<sup>39</sup> Spectra were processed and analyzed in Topspin, version 3.1 (Bruker BioSpin). A fragment library comprising ~13 800 compounds that generally satisfy the “rule of three” ( $\text{MW} \leq 300$ ,  $\text{cLogP} \leq 3.0$ , no more than three hydrogen bond donors)<sup>40</sup> and having no more than four rotatable bonds was screened as mixtures of 12 fragments. Samples (500  $\mu\text{L}$ ) contained 50  $\mu\text{M}$   $^{15}\text{N}$ -labeled Mcl-1, 400  $\mu\text{M}$  of each fragment, and 5% DMSO- $d_6$ . Deconvolution of hit mixtures was performed as single fragments. Recycling of the protein used for screening was accomplished by a simple buffer exchange with a yield of 50–80%.

NOE-derived distance restraints were acquired to enable NMR-based docking of fragments into a previously determined X-ray structure of a Mcl-1/peptide complex. Spectra were recorded on a Bruker 800 MHz



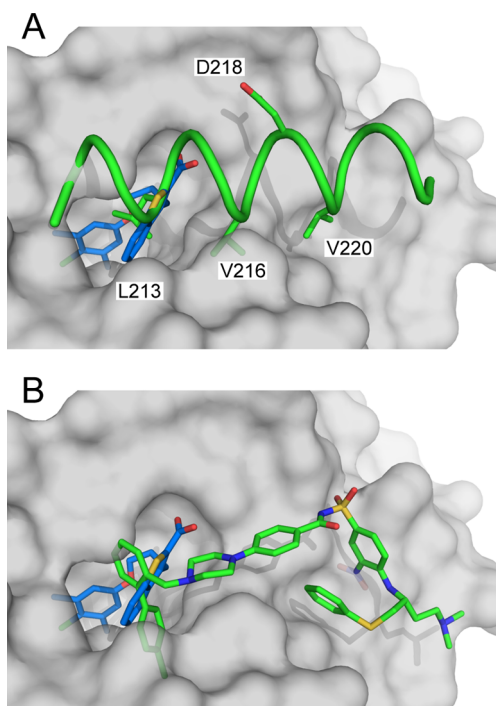


**Figure 6.** (A) Comparison of Mcl-1 (gray surface) when complexed to compound **60** (blue) and a 16-mer BH3-peptide derived from Mcl-1 (green). (B) Overlay of the X-ray structures of Mcl-1/**60** complex and Bcl-xL/ABT-737 (PDB code 2YXJ). The Mcl-1 protein is shown in gray, **60** in blue, and ABT-737 in green.

spectrometer equipped with a cryoprobe and pulsed field gradients. 300  $\mu\text{M}$   $^{15}\text{N}/^{13}\text{C}$ -labeled samples of Mcl-1 were prepared in a  $\text{D}_2\text{O}$ -based NMR buffer and mixed with selected fragments at 1 mM. Side chain  $^1\text{H}$  and  $^{13}\text{C}$  NMR signals were assigned from  $^{13}\text{C}$ -edited NOE and HCCH-TOCSY experiments.<sup>41</sup> NOE distance restraints were obtained from three-dimensional  $^{13}\text{C}$ -edited NOESY spectra, as well as three-dimensional  $^{15}\text{N}$ - and  $^{13}\text{C}$ -filter/edit NOESY spectra acquired with a mixing time of 80 ms. Compounds were docked into a X-ray structure

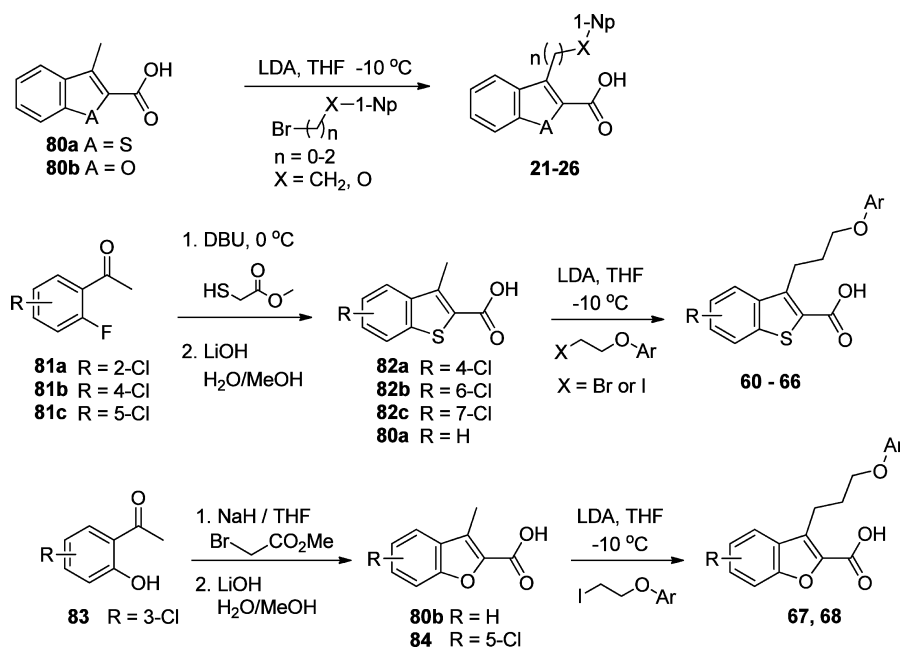
of a Mcl-1/BIM peptide complex (PDB code 3KJ2) using the NMR-derived restraints and a simulated annealing protocol using the program Xplor-NIH.<sup>35,42</sup> A square-well potential ( $F_{\text{NOE}} = 50 \text{ kcal mol}^{-1}$ ) was employed to constrain NOE-derived distances. Five low energy models from this process were energy minimized using MOE 2011.10 (Chemical Computing Group Inc., Montreal, Canada). The lowest energy structures obtained by this method were consistent with the observed NOEs.

**Protein Crystallization, Data Collection, and Structure Refinement.** Fresh batches of Mcl-1 proteins, WT and  $\Delta 5$ , were concentrated to 600  $\mu\text{M}$  (10.7 mg/mL) and 1 mM (17.4 mg/mL), respectively, and screened for crystallization conditions with a 1.2 $\times$  excess of ligand. Crystals were obtained by mixing 1  $\mu\text{L}$  of protein with 1  $\mu\text{L}$  of reservoir solution (25–30% PEG 3350, 0.1 M Bis-Tris, pH 6.5, 0.2 M  $\text{MgCl}_2$ ) as a hanging drop at 4 or 18  $^\circ\text{C}$ . Crystals appeared within the first week and were flash frozen in liquid nitrogen after cryoprotection using 10–20% glycol. Crystals of Mcl-1 bound to a 16-mer BH3-peptide derived from Mcl-1 itself (residues 209–224, Ac-ALETLRVGDGVQRNH-NH<sub>2</sub>, GenScript) were grown in a slightly different crystallization condition (25% PEG 3350, 0.1 M Bis-TRIS pH 5.5, 0.2 M NaCl). Crystals grew overnight at 18  $^\circ\text{C}$ .

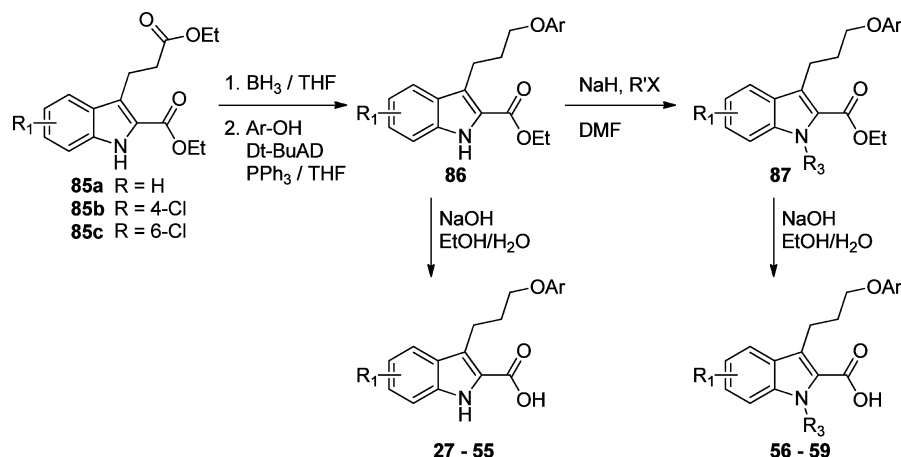
Data were collected on the Life Sciences Collaborative Access Team (LS-CAT) 21-ID-D beamline at the Advanced Photon Source (APS), Argonne National Laboratory. Indexing, integration, and scaling were performed with HKL2000.<sup>43</sup> By use of a previously determined peptide-bound structure (PDB code 3MK8), phasing was done by molecular replacement with Phaser<sup>44</sup> as implemented in CCP4.<sup>45</sup> Refinement of the structural models were performed with Phenix<sup>46</sup> and Refmac<sup>47</sup> and included rounds of manual model building in COOT.<sup>48</sup> Figures were prepared in PyMOL<sup>49</sup> and MOE.

**FPA Competition Assays.** Fluorescein isothiocyanate (FITC) labeled Mcl-1-BH3 peptide (FITC-AHx-KALETLRVGDGVQRNHETAF-NH<sub>2</sub>)<sup>23</sup> and FITC-Bak-BH3 peptide (FITC-AHx-GQVGRQLAIIGDDINR-NH<sub>2</sub>) were purchased from GenScript and used without further purification. FPA measurements were carried out in 384-well, black, flat-bottom plates (Greiner Bio-One) using the EnVision plate reader (PerkinElmer). All assays were conducted in assay buffer containing 20 mM Tris, pH 7.5, 50 mM NaCl, 3 mM DTT, and 2% DMSO. To measure inhibition of the Mcl-1/FITC-Mcl-1-BH3 interaction, Mcl-1 and FITC-Mcl-1-BH3 peptide were each added at 250 nM. To measure inhibition of the FITC-Bak-BH3 interaction with Bcl-2 family members, 10 nM FITC-Bak-BH3 peptide was incubated

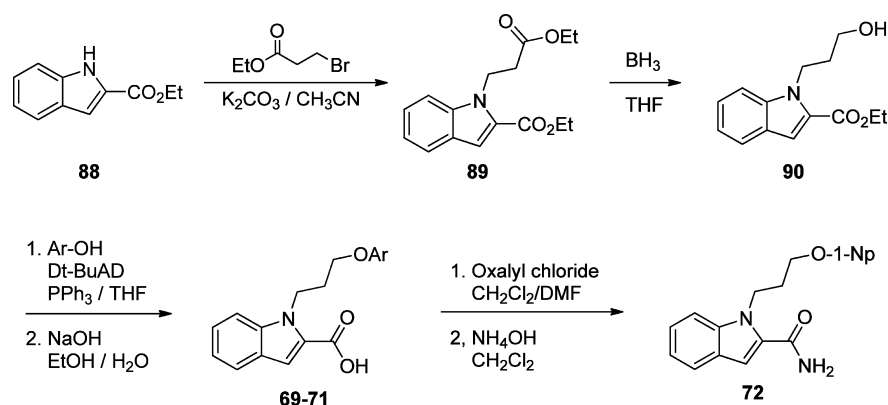
### Scheme 1. Synthesis of Benzothiophene- and Benzofuran-Containing Compounds



Scheme 2. Synthesis of Indole-Based Compounds



Scheme 3. Synthesis of Compounds 69–72



with either 14 nM Mcl-1, 4 nM Bcl-xL, or 40 nM Bcl-2. For  $IC_{50}$  determination, compounds were diluted in DMSO in a 16-point, 2-fold serial dilution scheme, added to assay plates, and incubated for 1 h at room temperature. The change in anisotropy was measured and used to calculate an  $IC_{50}$  (inhibitor concentration at which 50% of bound peptide is displaced) by fitting the inhibition data using XLFit software (Guildford, UK) to a single-site binding model. This was converted into a binding dissociation constant ( $K_i$ ) according to the formula<sup>50</sup>

$$K_i = [I]_{50} / ([L]_{50} / K_d^{pep} + [P]_0 / K_d^{pep} + 1)$$

where  $[I]_{50}$  is the concentration of the free inhibitor at 50% inhibition,  $[L]_{50}$  is the concentration of the free labeled ligand at 50% inhibition,  $[P]_0$  is the concentration of the free protein at 0% inhibition, and  $K_d^{pep}$  represents the dissociation constant of the FITC-labeled peptide probe.

**Chemistry. General.** All NMR spectra were recorded at room temperature on a 400 MHz AMX Bruker spectrometer.  $^1H$  chemical shifts are reported in  $\delta$  values in ppm downfield with the deuterated solvent as the internal standard. Data are reported as follows: chemical shift, multiplicity (s = singlet, d = doublet, t = triplet, q = quartet, br = broad, m = multiplet), integration, coupling constant (Hz). Low resolution mass spectra were obtained on an Agilent 1200 series 6140 mass spectrometer with electrospray ionization. All samples were of  $\geq 95\%$  purity as analyzed by LC–UV/vis–MS. Analytical HPLC was performed on an Agilent 1200 series with UV detection at 214 and 254 nm along with ELSD detection. LC–MS parameters were as follows: Phenomenex-C18 Kinetex column, 50 mm  $\times$  2.1 mm, 2 min gradient, 5% (0.1% TFA/MeCN)/95% (0.1% TFA/ $H_2O$ ) to 100% (0.1% TFA/MeCN). Preparative purification was performed on a Gilson HPLC (Phenomenex-C18, 100 mm  $\times$  30 mm, 10 min gradient, 5%  $\rightarrow$  95% MeCN/ $H_2O$  with 0.1% TFA) or by automated flash column chromatography (Isco, Inc. 100sg Combiflash). Solvents for extraction,

washing, and chromatography were HPLC grade. All reagents were purchased from chemical suppliers and used without purification.

**3-(2-(Naphthalen-1-yl)ethyl)benzo[*b*]thiophene-2-carboxylic Acid (21).** General Procedure for Alkylation of 3-Methylbenzothiophene or 3-Methylbenzofuran-2-carboxylic Acid. To a stirred solution of 3-methylbenzo[*b*]thiophene-2-carboxylic acid (101 mg, 0.53 mmol) in anhydrous THF (5.0 mL) was added LDA (0.58 mL, 1.17 mmol, 2 M in THF) dropwise under Ar at  $-10^\circ C$ . The reaction mixture was stirred for 30 min. Then a solution of 1-(bromomethyl)naphthalene (116 mg, 0.525 mmol) in THF (2 mL) was added dropwise. The reaction mixture was stirred for an additional 1 h at  $-10^\circ C$  and then warmed to room temperature and stirred overnight. The reaction was quenched by addition of saturated  $NH_4Cl$  aqueous solution and extracted with  $CH_2Cl_2$  (2  $\times$  20 mL). The organic extracts were combined, concentrated and the residue was purified by reverse phase preparative HPLC to give the product as a solid (103 mg, 0.310 mmol).  $^1H$  NMR (400 MHz,  $DMSO-d_6$ ):  $\delta$  (ppm) 8.37 (d,  $J = 8.2$  Hz, 1H), 8.02 (d,  $J = 8.0$  Hz, 1H), 7.93 (d,  $J = 8.0$  Hz, 2H), 7.79 (dd,  $J = 7.2$ , 1.8 Hz, 1H), 7.53 (m, 3H), 7.44 (m, 3H), 3.61 (m, 2H), 3.33 (m, 2H);  $>98\%$  at 215 nm, MS (ESI)  $m/z = 333.3$  ( $M + H$ )<sup>+</sup>.

**3-(3-(Naphthalen-1-yl)propyl)benzo[*b*]thiophene-2-carboxylic Acid (22).** The general procedure for alkylation was followed using 3-methylbenzo[*b*]thiophene-2-carboxylic acid (86 mg, 0.45 mmol) and 1-(2-bromoethyl)naphthalene (105 mg, 0.45 mmol) to yield the title compound (78 mg, 0.23 mmol).  $^1H$  NMR (400 MHz,  $DMSO-d_6$ ):  $\delta$  (ppm) 7.96 (m, 2H), 7.88 (m, 2H), 7.75 (d,  $J = 7.5$  Hz, 1H), 7.48 (m, 3H), 7.40 (m, 3H), 3.41 (t,  $J = 7.7$  Hz, 2H), 3.15 (t,  $J = 7.8$  Hz, 2H), 1.99 (p,  $J = 7.7$  Hz, 2H);  $>98\%$  at 215 nm, MS (ESI)  $m/z = 369.1$  ( $M + Na$ )<sup>+</sup>.

**3-(3-(Naphthalen-1-yloxy)propyl)benzo[*b*]thiophene-2-carboxylic Acid (23).** The general procedure for alkylation was followed using 3-methylbenzo[*b*]thiophene-2-carboxylic acid (100 mg, 0.52 mmol) and 1-(2-bromoethoxy)naphthalene (131 mg, 0.52 mmol) to

yield the title compound (101 mg, 0.28 mmol).  $^1\text{H}$  NMR (400 MHz,  $\text{DMSO}-d_6$ ):  $\delta$  (ppm) 8.18 (d,  $J = 7.8$  Hz, 1H), 8.01 (t,  $J = 7.9$  Hz, 2H), 7.85 (m, 1H), 7.48 (m, 4H), 7.37 (m, 2H), 6.89 (d,  $J = 7.4$  Hz, 1H), 4.21 (t,  $J = 5.9$ , 2H), 3.54 (t,  $J = 7.6$ , 2H), 2.20 (m, 2H); >98% at 215 nm, MS (ESI)  $m/z = 363.1$  ( $\text{M} + \text{H}$ ) $^+$ .

**3-(3-(4-Chloro-3,5-dimethylphenoxy)propyl)benzo[b]thiophene-2-carboxylic Acid (60).** The general procedure for alkylation was followed using 3-methylbenzo[b]thiophene-2-carboxylic acid (97 mg, 0.50 mmol) and 5-(2-bromoethoxy)-2-chloro-1,3-dimethylbenzene (133 mg, 0.50 mmol) to yield the title compound (89 mg, 0.24 mmol).  $^1\text{H}$  NMR (400 MHz,  $\text{DMSO}-d_6$ ):  $\delta$  (ppm) 8.00 (d,  $J = 8.1$  Hz, 1H), 7.96 (d,  $J = 8.1$  Hz, 1H), 7.50 (t,  $J = 7.5$  Hz, 1H), 7.42 (t,  $J = 7.6$  Hz, 1H), 6.74 (s, 2H), 3.98 (t,  $J = 6.2$  Hz, 2H), 3.38 (t,  $J = 7.5$ , 2H), 2.26 (s, 6H), 2.01 (p,  $J = 7.2$ , 2H); >98% at 215 nm, MS (ESI)  $m/z = 375.1$  ( $\text{M} + \text{H}$ ) $^+$ .

**4-Chloro-3-(3-(4-chloro-3,5-dimethylphenoxy)propyl)benzo[b]thiophene-2-carboxylic Acid (61).** The general procedure for alkylation was followed using 4-chloro-3-methylbenzo[b]thiophene-2-carboxylic acid (57 mg, 0.25 mmol) and 2-chloro-5-(2-iodoethoxy)-1,3-dimethylbenzene (78 mg, 0.25 mmol) to yield the title compound (25.6 mg, 0.063 mmol).  $^1\text{H}$  NMR (400 MHz,  $\text{DMSO}-d_6$ ):  $\delta$  (ppm) 8.01 (dd,  $J = 7.7$ , 1.1 Hz, 1H), 7.49 (m, 2H), 6.73 (s, 2H), 4.05 (t,  $J = 6.2$  Hz, 2H), 3.70 (m, 2H), 2.26 (s, 6H), 2.05 (m, 2H); >98% at 215 nm, MS (ESI)  $m/z = 409.1$  ( $\text{M} + \text{H}$ ) $^+$ .

**4-Chloro-3-(3-(naphthalen-1-yloxy)propyl)benzo[b]thiophene-2-carboxylic Acid (62).** The general procedure for alkylation was followed using 4-chloro-3-methylbenzo[b]thiophene-2-carboxylic acid (57 mg, 0.25 mmol) and 1-(2-iodoethoxy)naphthalene (75 mg, 0.25 mmol) to yield the title compound (9.9 mg, 0.025 mmol).  $^1\text{H}$  NMR (400 MHz,  $\text{DMSO}-d_6$ ):  $\delta$  (ppm) 8.15 (d,  $J = 8.0$  Hz, 1H), 8.02 (m, 1H), 7.85 (d,  $J = 7.9$  Hz, 1H), 7.46 (m, 6H), 6.96 (d,  $J = 7.2$  Hz, 1H), 4.28 (t,  $J = 5.9$ , 2H), 3.87 (m, 2H), 2.23 (m, 2H); >98% at 215 nm, MS (ESI)  $m/z = 419.1$  ( $\text{M} + \text{Na}$ ) $^+$ .

**6-Chloro-3-(3-(4-chloro-3,5-dimethylphenoxy)propyl)benzo[b]thiophene-2-carboxylic Acid (63).** The general procedure for alkylation was followed using 6-chloro-3-methylbenzo[b]thiophene-2-carboxylic acid (57 mg, 0.25 mmol) and 2-chloro-5-(2-iodoethoxy)-1,3-dimethylbenzene (78 mg, 0.25 mmol) to yield the title compound (36 mg, 0.087 mmol).  $^1\text{H}$  NMR (400 MHz,  $\text{DMSO}-d_6$ ):  $\delta$  (ppm) 8.18 (d,  $J = 1.9$  Hz, 1H), 7.97 (d,  $J = 8.7$  Hz, 1H), 7.45 (dd,  $J = 8.7$ , 1.9 Hz, 1H), 6.70 (s, 2H), 3.96 (t,  $J = 6.2$  Hz, 2H), 3.36 (m, 2H), 2.26 (s, 6H), 2.00 (p,  $J = 7.2$  Hz, 2H); >98% at 215 nm, MS (ESI)  $m/z = 431.1$  ( $\text{M} + \text{Na}$ ) $^+$ .

**6-Chloro-3-(3-(naphthalen-1-yloxy)propyl)benzo[b]thiophene-2-carboxylic Acid (64).** The general procedure for alkylation was followed using 6-chloro-3-methylbenzo[b]thiophene-2-carboxylic acid (57 mg, 0.25 mmol) and 1-(2-iodoethoxy)naphthalene (75 mg, 0.25 mmol) to yield the title compound (9.9 mg, 0.025 mmol).  $^1\text{H}$  NMR (400 MHz,  $\text{DMSO}-d_6$ ):  $\delta$  (ppm) 8.17 (d,  $J = 1.9$  Hz, 1H), 8.12 (d,  $J = 8.0$  Hz, 1H), 8.02 (d,  $J = 8.8$  Hz, 1H), 7.84 (d,  $J = 7.7$  Hz, 1H), 7.48 (m, 3H), 7.38 (m, 2H), 6.89 (d,  $J = 7.4$  Hz, 1H), 4.20 (t,  $J = 5.9$ , 2H), 3.52 (t,  $J = 7.6$ , 2H), 2.18 (m, 2H); >98% at 215 nm, MS (ESI)  $m/z = 419.1$  ( $\text{M} + \text{Na}$ ) $^+$ .

**7-Chloro-3-(3-(4-chloro-3,5-dimethylphenoxy)propyl)benzo[b]thiophene-2-carboxylic Acid (65).** The general procedure for alkylation was followed using 7-chloro-3-methylbenzo[b]thiophene-2-carboxylic acid (57 mg, 0.25 mmol) and 2-chloro-5-(2-iodoethoxy)-1,3-dimethylbenzene (78 mg, 0.25 mmol) to yield the title compound (53 mg, 0.13 mmol).  $^1\text{H}$  NMR (400 MHz,  $\text{DMSO}-d_6$ ):  $\delta$  (ppm) 7.97 (d,  $J = 8.1$  Hz, 1H), 7.64 (d,  $J = 7.6$  Hz, 1H), 7.47 (t,  $J = 7.9$  Hz, 1H), 6.70 (s, 2H), 3.97 (t,  $J = 6.1$  Hz, 2H), 3.38 (m, 2H), 2.25 (s, 6H), 2.02 (p,  $J = 7.1$  Hz, 2H); MS (ESI)  $m/z = 409.1$  ( $\text{M} + \text{H}$ ) $^+$ .

**7-Chloro-3-(3-(naphthalen-1-yloxy)propyl)benzo[b]thiophene-2-carboxylic Acid (66).** The general procedure for alkylation was followed using 7-chloro-3-methylbenzo[b]thiophene-2-carboxylic acid (57 mg, 0.25 mmol) and 1-(2-iodoethoxy)naphthalene (75 mg, 0.25 mmol) to yield the title compound (25 mg, 0.062 mmol).  $^1\text{H}$  NMR (400 MHz,  $\text{DMSO}-d_6$ ):  $\delta$  (ppm) 8.05 (d,  $J = 8.2$  Hz, 1H), 8.02 (d,  $J = 8.1$  Hz, 1H), 7.84 (d,  $J = 8.0$  Hz, 1H), 7.61 (d,  $J = 7.6$  Hz, 1H), 7.50 (m, 1H), 7.41 (m, 4H), 6.88 (d,  $J = 7.5$  Hz, 1H), 4.20 (t,  $J = 5.8$ ,

2H), 3.54 (t,  $J = 7.5$ , 2H), 2.21 (p,  $J = 7.1$  Hz, 2H); MS (ESI)  $m/z = 397.0$  ( $\text{M} + \text{H}$ ) $^+$ .

**3-(3-(Naphthalen-1-yl)propyl)benzofuran-2-carboxylic Acid (24).** The general procedure for alkylation was followed using 3-methylbenzofuran-2-carboxylic acid and 1-(bromomethyl)naphthalene to yield the title compound.  $^1\text{H}$  NMR (400 MHz,  $\text{CDCl}_3$ ):  $\delta$  (ppm) 8.26 (d, 1H,  $J = 8.4$  Hz), 7.91 (d, 1H,  $J = 8.4$  Hz), 7.75 (d, 1H,  $J = 8.2$  Hz), 7.32–7.62 (m, 8H), 3.48–3.59 (m, 4H); >98% at 215 nm, MS (ESI)  $m/z = 317.0$  ( $\text{M} + \text{H}$ ) $^+$ .

**3-(2-(nNaphthalen-1-yl)ethyl)benzofuran-2-carboxylic Acid (25).** The general procedure for alkylation was followed using 3-methylbenzofuran-2-carboxylic acid and 1-(2-bromoethyl)naphthalene to yield the title compound.  $^1\text{H}$  NMR (400 MHz,  $\text{CDCl}_3$ ):  $\delta$  (ppm) 8.26 (d, 1H,  $J = 8.6$  Hz), 7.32–7.97 (m, 10H), 3.42–3.59 (m, 2H), 3.17–3.36 (m, 2H), 2.18–2.30 (m, 2H); >98% at 215 nm, MS (ESI)  $m/z = 331.0$  ( $\text{M} + \text{H}$ ) $^+$ .

**3-(3-(Naphthalen-1-yloxy)propyl)benzofuran-2-carboxylic Acid (26).** The general procedure for alkylation was followed using 3-methylbenzofuran-2-carboxylic acid and 1-(2-bromoethoxy)naphthalene to yield the title compound.  $^1\text{H}$  NMR (400 MHz,  $\text{CDCl}_3$ ):  $\delta$  (ppm) 8.26 (d, 1H,  $J = 8.6$  Hz), 7.32–7.97 (m, 10H), 4.01 (m, 2H), 3.32 (m, 2H), 2.28 (m, 2H); >98% at 215 nm, MS (ESI)  $m/z = 347.2$  ( $\text{M} + \text{H}$ ) $^+$ .

**3-(3-(4-Chloro-3,5-dimethylphenoxy)propyl)benzofuran-2-carboxylic Acid (67).** The general procedure for alkylation was followed using 3-methylbenzofuran-2-carboxylic acid and 2-chloro-5-(2-bromoethoxy)-1,3-dimethylbenzene to yield the title compound.  $^1\text{H}$  NMR (400 MHz,  $\text{CDCl}_3$ ):  $\delta$  (ppm) 7.71 (d,  $J = 8.4$  Hz, 1H), 7.59 (d,  $J = 8.6$  Hz, 1H), 7.49–7.54 (m, 1H), 7.28–7.34 (m, 1H), 6.62 (s, 2H), 3.99 (t,  $J = 6.0$  Hz, 2H), 3.32 (t,  $J = 7.4$  Hz, 2H), 2.34 (s, 6H), 2.23 (m, 2H); >98% at 215 nm, MS (ESI)  $m/z = 359.1$  ( $\text{M} + \text{H}$ ) $^+$ .

**5-Chloro-3-(3-(naphthalen-1-yloxy)propyl)benzofuran-2-carboxylic Acid (68).** The general procedure for alkylation was followed using 5-chloro-3-methylbenzofuran-2-carboxylic acid<sup>51</sup> and 1-(2-bromoethoxy)naphthalene to yield the title compound: >98% at 215 nm, MS (ESI)  $m/z = 381.1$  ( $\text{M} + \text{H}$ ) $^+$ .

**3-(3-Phenoxypropyl)-1H-indole-2-carboxylic Acid (27). General Procedure for Phenol Analogue Coupling and Saponification.** To a solution of ethyl 3-(3-hydroxypropyl)-1H-indole-2-carboxylate (70 mg, 0.28 mmol),  $\text{PPh}_3$  (110 mg, 0.51 mmol), and phenol (49 mg, 0.52 mmol) in THF (3.5 mL) was added  $\text{Dt-BuAD}$  (99 mg, 0.51 mmol) at 20 °C. The reaction mixture was stirred for 15 h at 20 °C and then concentrated in vacuo. The residue was purified by flash chromatography (Combi-flash Rf hexane/EtOAc gradient 0–10%) to give ethyl 3-(3-phenoxypropyl)-1H-indole-2-carboxylic acid, the title compound (92 mg, 0.25 mmol), as a colorless oil: >98% at 215 nm, MS (ESI)  $m/z = 324.1$  ( $\text{M} + \text{H}$ ) $^+$ .

To a solution of the ethyl ester (28 mg, 0.085 mmol) in EtOH (1.0 mL) was added 50%  $\text{NaOH}-\text{H}_2\text{O}$  solution (50  $\mu\text{L}$ ) at 20 °C. The reaction mixture was stirred for 15 h at 20 °C. The reaction mixture was acidified with 1 N  $\text{HCl}$  solution, extracted with EtOAc, dried over  $\text{MgSO}_4$ , filtered, and concentrated in vacuo. The crude product was purified by reverse phase preparative HPLC ( $\text{H}_2\text{O}/\text{CH}_3\text{CN}$  gradient to 95%  $\text{CH}_3\text{CN}/0.5\%$  TFA) to yield the title compound (23 mg, 0.078 mmol) as a white solid.  $^1\text{H}$  NMR (400 MHz,  $\text{DMSO}-d_6$ ):  $\delta$  (ppm) 11.43 (s, 1H), 7.64 (d,  $J = 8.0$  Hz, 1H), 7.39 (d,  $J = 8.4$  Hz, 1H), 7.20–7.31 (m, 3H), 7.00 (t,  $J = 7.2$  Hz, 1H), 6.89–6.99 (m, 3H), 3.95 (t,  $J = 6.4$  Hz, 2H), 3.21 (t,  $J = 6.4$  Hz, 2H), 2.01–2.10 (m, 2H); >98% at 215 nm, MS (ESI)  $m/z = 296.1$  [ $\text{M} + \text{H}$ ] $^+$ .

Compounds 28–55 were prepared following the general procedure outlined above in library format. Purity of all final compounds was determined by HPLC analysis and is >95%. All compounds were isolated as solids.

**3-(3-(o-Tolyloxy)propyl)-1H-indole-2-carboxylic Acid (28).** Coupling of ethyl 3-(3-hydroxypropyl)-1H-indole-2-carboxylate and *o*-cresol yielded 28.  $^1\text{H}$  NMR (400 MHz,  $\text{DMSO}-d_6$ ):  $\delta$  (ppm) 11.39 (s, 1H), 7.64 (d,  $J = 8.0$  Hz, 1H), 7.40 (d,  $J = 8.4$  Hz, 1H), 7.22 (t,  $J = 7.2$  Hz, 1H), 7.13 (t,  $J = 8.0$  Hz, 1H), 7.02 (t,  $J = 7.2$  Hz, 1H), 6.67–6.76 (m, 3H), 3.94 (t,  $J = 6.4$  Hz, 2H), 3.20 (t,  $J = 6.4$  Hz, 2H), 2.25 (s, 3H), 2.01–2.11 (m, 2H); >98% at 215 nm, MS (ESI)  $m/z = 310.1$  [ $\text{M} + \text{H}$ ] $^+$ .



**3-(3-(2-(Trifluoromethyl)phenoxy)propyl)-1H-indole-2-carboxylic Acid (29).** Coupling of ethyl 3-(3-hydroxypropyl)-1H-indole-2-carboxylate and 2-(trifluoromethyl)phenol yielded 29. <sup>1</sup>H NMR (400 MHz, DMSO-*d*<sub>6</sub>):  $\delta$  (ppm) 11.43 (s, 1H), 7.64 (d, *J* = 8.0 Hz, 1H), 7.50 (t, *J* = 7.2 Hz, 1H), 7.39 (d, *J* = 8.4 Hz, 1H), 7.16–7.35 (m, 4H), 6.98 (t, *J* = 7.2 Hz, 1H), 4.04 (t, *J* = 6.4 Hz, 2H), 3.22 (t, *J* = 6.4 Hz, 2H), 2.01–2.12 (m, 2H); >98% at 215 nm, MS (ESI) *m/z* = 364.1 [M + H]<sup>+</sup>.

**3-(3-(*m*-Tolyloxy)propyl)-1H-indole-2-carboxylic Acid (30).** Coupling of ethyl 3-(3-hydroxypropyl)-1H-indole-2-carboxylate and *m*-cresol yielded 30. <sup>1</sup>H NMR (400 MHz, DMSO-*d*<sub>6</sub>):  $\delta$  (ppm) 11.39 (s, 1H), 7.64 (d, *J* = 8.0 Hz, 1H), 7.40 (d, *J* = 8.4 Hz, 1H), 7.22 (t, *J* = 7.2 Hz, 1H), 7.13 (t, *J* = 8.0 Hz, 1H), 7.02 (t, *J* = 7.2 Hz, 1H), 6.67–6.76 (m, 3H), 3.94 (t, *J* = 6.4 Hz, 2H), 3.20 (t, *J* = 6.4 Hz, 2H), 2.25 (s, 3H), 2.01–2.11 (m, 2H); >98% at 215 nm, MS (ESI) *m/z* = 310.1 [M + H]<sup>+</sup>.

**3-(3-(3-(Trifluoromethyl)phenoxy)propyl)-1H-indole-2-carboxylic Acid (31).** Coupling of ethyl 3-(3-hydroxypropyl)-1H-indole-2-carboxylate and 3-(trifluoromethyl)phenol yielded 31. <sup>1</sup>H NMR (400 MHz, DMSO-*d*<sub>6</sub>):  $\delta$  (ppm) 11.43 (s, 1H), 7.64 (d, *J* = 8.0 Hz, 1H), 7.50 (t, *J* = 7.2 Hz, 1H), 7.39 (d, *J* = 8.4 Hz, 1H), 7.16–7.35 (m, 4H), 6.98 (t, *J* = 7.2 Hz, 1H), 4.04 (t, *J* = 6.4 Hz, 2H), 3.22 (t, *J* = 6.4 Hz, 2H), 2.01–2.12 (m, 2H); >98% at 215 nm, MS (ESI) *m/z* = 364.1 [M + H]<sup>+</sup>.

**3-(3-(*p*-Tolyloxy)propyl)-1H-indole-2-carboxylic Acid (32).** Coupling of ethyl 3-(3-hydroxypropyl)-1H-indole-2-carboxylate and *p*-cresol yielded 32. <sup>1</sup>H NMR (400 MHz, DMSO-*d*<sub>6</sub>):  $\delta$  (ppm) 11.41 (s, 1H), 7.63 (d, *J* = 8.0 Hz, 1H), 7.39 (d, *J* = 8.0 Hz, 1H), 7.22 (t, *J* = 7.2 Hz, 1H), 7.06 (d, *J* = 8.0 Hz, 2H), 7.02 (t, *J* = 7.2 Hz, 1H), 6.79 (d, *J* = 8.4 Hz, 2H), 3.91 (t, *J* = 6.4 Hz, 2H), 3.19 (t, *J* = 6.4 Hz, 2H), 2.22 (s, 3H), 1.98–2.09 (m, 2H); >98% at 215 nm, MS (ESI) *m/z* = 310.1 [M + H]<sup>+</sup>.

**3-(3-(4-Chlorophenoxy)propyl)-1H-indole-2-carboxylic Acid (33).** Coupling of ethyl 3-(3-hydroxypropyl)-1H-indole-2-carboxylate and 4-chlorophenol yielded 33. <sup>1</sup>H NMR (400 MHz, DMSO-*d*<sub>6</sub>):  $\delta$  (ppm) 11.42 (s, 1H), 7.63 (d, *J* = 8.0 Hz, 1H), 7.39 (d, *J* = 8.4 Hz, 1H), 7.30 (d, *J* = 8.8 Hz, 2H), 7.22 (t, *J* = 7.2 Hz, 1H), 6.99 (t, *J* = 7.2 Hz, 1H), 6.93 (d, *J* = 8.8 Hz, 2H), 3.94 (t, *J* = 6.4 Hz, 2H), 3.19 (t, *J* = 6.4 Hz, 2H), 2.00–2.10 (m, 2H); >98% at 215 nm, MS (ESI) *m/z* = 330.1 [M + H]<sup>+</sup>.

**3-(3-(4-(Trifluoromethyl)phenoxy)propyl)-1H-indole-2-carboxylic Acid (34).** Coupling of ethyl 3-(3-hydroxypropyl)-1H-indole-2-carboxylate and 4-(trifluoromethyl)phenol yielded 34. <sup>1</sup>H NMR (400 MHz, DMSO-*d*<sub>6</sub>):  $\delta$  (ppm) 11.43 (s, 1H), 7.60–7.69 (m, 3H), 7.39 (d, *J* = 8.4 Hz, 1H), 7.22 (t, *J* = 7.2 Hz, 1H), 7.08 (d, *J* = 8.4 Hz, 2H), 6.99 (t, *J* = 7.2 Hz, 1H), 4.04 (t, *J* = 6.4 Hz, 2H), 3.22 (t, *J* = 6.4 Hz, 2H), 2.03–2.13 (m, 2H); >98% at 215 nm, MS (ESI) *m/z* = 364.1 [M + H]<sup>+</sup>.

**3-(3-(4-Chloro-3-methylphenoxy)propyl)-1H-indole-2-carboxylic Acid (35).** Coupling of ethyl 3-(3-hydroxypropyl)-1H-indole-2-carboxylate and 4-chloro-3-methylphenol yielded 35. <sup>1</sup>H NMR (400 MHz, DMSO-*d*<sub>6</sub>):  $\delta$  (ppm) 11.42 (s, 1H), 7.63 (d, *J* = 8.0 Hz, 1H), 7.39 (d, *J* = 8.4 Hz, 1H), 7.18–7.30 (m, 2H), 7.00 (t, *J* = 7.6 Hz, 1H), 6.85 (s, 1H), 6.75 (d, *J* = 8.4 Hz, 1H), 3.94 (t, *J* = 6.4 Hz, 2H), 3.19 (t, *J* = 6.8 Hz, 2H), 2.24 (s, 3H), 1.95–2.10 (m, 2H); >98% at 215 nm, MS (ESI) *m/z* = 344.1 [M + H]<sup>+</sup>.

**3-(3-(4-Chloro-3-ethylphenoxy)propyl)-1H-indole-2-carboxylic Acid (36).** Coupling of ethyl 3-(3-hydroxypropyl)-1H-indole-2-carboxylate and 4-chloro-3-ethylphenol yielded 36. <sup>1</sup>H NMR (400 MHz, DMSO-*d*<sub>6</sub>):  $\delta$  (ppm) 11.42 (s, 1H), 7.63 (d, *J* = 8.0 Hz, 1H), 7.39 (d, *J* = 8.4 Hz, 1H), 7.26 (d, *J* = 8.8 Hz, 1H), 7.22 (t, *J* = 8.0 Hz, 1H), 7.02 (t, *J* = 8.0 Hz, 1H), 6.87 (s, 1H), 6.76 (d, *J* = 8.8 Hz, 1H), 3.95 (t, *J* = 6.4 Hz, 2H), 3.20 (t, *J* = 6.8 Hz, 2H), 2.61 (q, *J* = 7.6 Hz, 2H), 1.95–2.10 (m, 2H), 1.15 (t, *J* = 7.6 Hz, 3H); >98% at 215 nm, MS (ESI) *m/z* = 358.1 [M + H]<sup>+</sup>.

**3-(3-(4-Chloro-3,5-dimethylphenoxy)propyl)-1H-indole-2-carboxylic Acid (37).** Coupling of ethyl 3-(3-hydroxypropyl)-1H-indole-2-carboxylate and 4-chloro-3,5-dimethylphenol yielded 37. <sup>1</sup>H NMR (400 MHz, DMSO-*d*<sub>6</sub>):  $\delta$  (ppm) 11.42 (s, 1H), 7.63 (d, *J* = 8.0 Hz, 1H), 7.39 (d, *J* = 8.4 Hz, 1H), 7.22 (t, *J* = 7.6 Hz, 1H), 7.00 (t, *J* = 7.6 Hz, 1H), 6.74 (s, 2H), 3.93 (t, *J* = 6.4 Hz, 2H), 3.19 (t, *J* = 6.8 Hz, 2H), 2.27 (s, 6H), 1.95–2.10 (m, 2H); >98% at 215 nm, MS (ESI) *m/z* = 358.1 [M + H]<sup>+</sup>.

**3-(3-([1,1'-Biphenyl]-3-yloxy)propyl)-1H-indole-2-carboxylic Acid (38).** Coupling of ethyl 3-(3-hydroxypropyl)-1H-indole-2-carboxylate and [1,1'-biphenyl]-3-ol yielded 38. <sup>1</sup>H NMR (400 MHz, DMSO-*d*<sub>6</sub>):  $\delta$  (ppm) 11.43 (s, 1H), 7.55–7.75 (m, 3H), 7.31–7.52 (m,

5H), 7.25–7.46 (m, 3H), 6.98–7.03 (m, 1H), 6.91 (d, *J* = 8.0 Hz, 1H), 4.05 (t, *J* = 6.4 Hz, 2H), 3.23 (t, *J* = 6.4 Hz, 2H), 2.01–2.10 (m, 2H); >98% at 215 nm, MS (ESI) *m/z* = 372.1 [M + H]<sup>+</sup>.

**3-(3-([1,1'-Biphenyl]-4-yloxy)propyl)-1H-indole-2-carboxylic Acid (39).** Coupling of ethyl 3-(3-hydroxypropyl)-1H-indole-2-carboxylate and [1,1'-biphenyl]-4-ol yielded 39. <sup>1</sup>H NMR (400 MHz, DMSO-*d*<sub>6</sub>):  $\delta$  (ppm) 11.42 (s, 1H), 7.66 (d, *J* = 8.0 Hz, 1H), 7.63–7.52 (m, 4H), 7.35–7.45 (m, 4H), 7.32 (t, *J* = 7.2 Hz, 1H), 7.22 (t, *J* = 7.2 Hz, 1H), 6.95–7.05 (m, 2H), 4.01 (t, *J* = 6.4 Hz, 2H), 3.23 (t, *J* = 6.4 Hz, 2H), 2.03–2.13 (m, 2H); >98% at 215 nm, MS (ESI) *m/z* = 372.2 [M + H]<sup>+</sup>.

**3-(3-(3-Phenoxyphenoxy)propyl)-1H-indole-2-carboxylic Acid (40).** Coupling of ethyl 3-(3-hydroxypropyl)-1H-indole-2-carboxylate and 3-phenoxyphenol yielded 40. <sup>1</sup>H NMR (400 MHz, DMSO-*d*<sub>6</sub>):  $\delta$  (ppm) 11.42 (s, 1H), 7.61 (d, *J* = 8.4 Hz, 1H), 7.33–7.42 (m, 2H), 7.20–7.31 (m, 4H), 7.16 (t, *J* = 7.2 Hz, 1H), 6.95–7.05 (m, 3H), 6.69 (d, *J* = 7.6 Hz, 1H), 6.52 (s, 1H), 3.93 (t, *J* = 6.4 Hz, 2H), 3.19 (t, *J* = 6.4 Hz, 2H), 1.95–2.10 (m, 2H); >98% at 215 nm, MS (ESI) *m/z* = 388.2 [M + H]<sup>+</sup>.

**3-(3-(4-Phenoxyphenoxy)propyl)-1H-indole-2-carboxylic Acid (41).** Coupling of ethyl 3-(3-hydroxypropyl)-1H-indole-2-carboxylate and 4-phenoxyphenol yielded 41. <sup>1</sup>H NMR (400 MHz, DMSO-*d*<sub>6</sub>):  $\delta$  (ppm) 11.42 (s, 1H), 7.64 (d, *J* = 8.0 Hz, 1H), 7.32–7.45 (m, 3H), 7.23 (t, *J* = 8.0 Hz, 1H), 7.09 (t, *J* = 7.6 Hz, 1H), 6.90–7.03 (m, 7H), 3.95 (t, *J* = 6.4 Hz, 2H), 3.21 (t, *J* = 6.8 Hz, 2H), 2.02–2.10 (m, 2H); >98% at 215 nm, MS (ESI) *m/z* = 388.2 [M + H]<sup>+</sup>.

**3-(3-(Naphthalen-1-yloxy)propyl)-1H-indole-2-carboxylic Acid (42).** Coupling of ethyl 3-(3-hydroxypropyl)-1H-indole-2-carboxylate and 1-naphthol yielded 42. <sup>1</sup>H NMR (400 MHz, DMSO-*d*<sub>6</sub>):  $\delta$  (ppm) 11.60 (s, 1H), 8.24 (d, *J* = 6.8 Hz, 1H), 7.87 (d, *J* = 7.2 Hz, 1H), 7.66 (d, *J* = 8.0 Hz, 1H), 7.30–7.55 (m, 5H), 7.25 (t, *J* = 8.0 Hz, 1H), 6.95 (t, *J* = 7.6 Hz, 1H), 6.87 (d, *J* = 7.6 Hz, 1H), 4.16 (t, *J* = 6.0 Hz, 2H), 3.30–3.40 (m, 2H), 2.15–2.25 (m, 2H); >98% at 215 nm, MS (ESI) *m/z* = 346.1 [M + H]<sup>+</sup>.

**3-(3-(Naphthalen-2-yloxy)propyl)-1H-indole-2-carboxylic Acid (43).** Coupling of ethyl 3-(3-hydroxypropyl)-1H-indole-2-carboxylate and 2-naphthol yielded 43. <sup>1</sup>H NMR (400 MHz, DMSO-*d*<sub>6</sub>):  $\delta$  (ppm) 11.42 (s, 1H), 7.82 (d, *J* = 8.8 Hz, 1H), 7.73 (d, *J* = 8.0 Hz, 1H), 7.67 (d, *J* = 8.0 Hz, 1H), 7.35–7.52 (m, 3H), 7.34 (d, *J* = 7.2 Hz, 1H), 7.17–7.27 (2H, m), 6.98 (t, *J* = 7.2 Hz, 1H), 4.09 (t, *J* = 6.4 Hz, 2H), 3.26 (t, *J* = 6.4 Hz, 2H), 2.10–2.18 (m, 2H); >98% at 215 nm, MS (ESI) *m/z* = 346.1 [M + H]<sup>+</sup>.

**3-(3-((4-Chloronaphthalen-1-yl)oxy)propyl)-1H-indole-2-carboxylic Acid (44).** Coupling of ethyl 3-(3-hydroxypropyl)-1H-indole-2-carboxylate and 4-chloronaphthalen-1-ol yielded 44. <sup>1</sup>H NMR (400 MHz, DMSO-*d*<sub>6</sub>):  $\delta$  (ppm) 11.47 (s, 1H), 8.30 (d, *J* = 8.0 Hz, 1H), 8.11 (d, *J* = 8.0 Hz, 1H), 7.73 (t, *J* = 7.2 Hz, 1H), 7.62–7.69 (m, 2H), 7.56 (d, *J* = 8.4 Hz, 1H), 7.40 (d, *J* = 8.4 Hz, 1H), 7.21 (t, *J* = 7.2 Hz, 1H), 6.95 (t, *J* = 7.2 Hz, 1H), 6.88 (d, *J* = 8.4 Hz, 1H), 4.17 (t, *J* = 6.4 Hz, 2H), 3.28–2.35 (m, 2H), 2.17–2.27 (m, 2H); >98% at 215 nm, MS (ESI) *m/z* = 380.1 [M + H]<sup>+</sup>.

**3-(3-((5,6,7,8-Tetrahydronaphthalen-1-yl)oxy)propyl)-1H-indole-2-carboxylic Acid (45).** Coupling of ethyl 3-(3-hydroxypropyl)-1H-indole-2-carboxylate and 5,6,7,8-tetrahydronaphthalen-1-ol yielded 45. <sup>1</sup>H NMR (400 MHz, DMSO-*d*<sub>6</sub>):  $\delta$  (ppm) 11.42 (s, 1H), 7.63 (d, *J* = 8.0 Hz, 1H), 7.40 (d, *J* = 8.0 Hz, 1H), 7.20–7.28 (m, 1H), 6.92–7.07 (m, 2H), 6.60–6.70 (m, 2H), 3.94 (t, *J* = 6.4 Hz, 2H), 3.23 (t, *J* = 6.4 Hz, 2H), 2.69 (t, *J* = 0.60 Hz, 2H), 2.63 (t, *J* = 0.60 Hz, 2H), 2.01–2.10 (m, 2H), 1.63–1.80 (m, 4H); >98% at 215 nm, MS (ESI) *m/z* = 350.2 [M + H]<sup>+</sup>.

**3-(3-((2,3-Dihydro-1H-inden-5-yl)oxy)propyl)-1H-indole-2-carboxylic Acid (46).** Coupling of ethyl 3-(3-hydroxypropyl)-1H-indole-2-carboxylate and 2,3-dihydro-1H-inden-5-ol yielded 46. <sup>1</sup>H NMR (400 MHz, DMSO-*d*<sub>6</sub>):  $\delta$  (ppm) 11.42 (s, 1H), 7.64 (d, *J* = 8.0 Hz, 1H), 7.39 (d, *J* = 8.4 Hz, 1H), 7.22 (t, *J* = 7.6 Hz, 1H), 7.08 (d, *J* = 8.4 Hz, 1H), 7.03 (t, *J* = 7.6 Hz, 1H), 6.75 (s, 1H), 6.65–6.70 (d, *J* = 8.4 Hz, 1H), 3.91 (t, *J* = 6.4 Hz, 2H), 3.33 (t, *J* = 6.4 Hz, 2H), 2.70–2.83 (m, 4H), 1.90–2.10 (m, 4H); >98% at 215 nm, MS (ESI) *m/z* = 336.1 [M + H]<sup>+</sup>.

**3-(3-(Quinolin-6-yloxy)propyl)-1H-indole-2-carboxylic Acid (47).** Coupling of ethyl 3-(3-hydroxypropyl)-1H-indole-2-carboxylate



and quinolin-6-ol yielded **47**.  $^1\text{H}$  NMR (400 MHz, DMSO- $d_6$ ):  $\delta$  (ppm) 11.47 (s, 1H), 8.92 (d,  $J$  = 4.0 Hz, 1H), 8.53 (d,  $J$  = 8.0 Hz, 1H), 8.04 (d,  $J$  = 9.2 Hz, 1H), 7.72 (d,  $J$  = 8.0 Hz, 1H), 7.66 (d,  $J$  = 8.0 Hz, 1H), 7.61 (d,  $J$  = 9.2 Hz, 1H), 7.46 (s, 1H), 7.40 (d,  $J$  = 8.4 Hz, 1H), 7.61 (d,  $J$  = 9.2 Hz, 1H), 7.21 (t,  $J$  = 8.0 Hz, 1H), 6.97 (t,  $J$  = 8.0 Hz, 1H), 4.14 (t,  $J$  = 6.4 Hz, 2H), 3.26 (t,  $J$  = 7.2 Hz, 2H), 2.14–1.93 (m, 2H); >98% at 215 nm, MS (ESI)  $m/z$  = 347.1  $[\text{M} + \text{H}]^+$ .

**3-(3-((1H-indol-4-yl)oxy)propyl)-1H-indole-2-carboxylic Acid (48)**. Coupling of ethyl 3-(3-hydroxypropyl)-1H-indole-2-carboxylate and quinolin-6-ol yielded **48**.  $^1\text{H}$  NMR (400 MHz, DMSO- $d_6$ ):  $\delta$  (ppm) 11.45 (s, 1H), 11.04 (s, 1H), 7.68 (d,  $J$  = 8.0 Hz, 1H), 7.40 (d,  $J$  = 7.8 Hz, 1H), 7.15–7.30 (m, 2H), 6.91–7.07 (m, 3H), 6.48 (s, 1H), 6.39 (d,  $J$  = 7.2 Hz, 1H), 4.08 (t,  $J$  = 6.0 Hz, 2H), 3.26 (t,  $J$  = 6.0 Hz, 2H), 2.09–2.20 (m, 2H); >98% at 215 nm, MS (ESI)  $m/z$  = 335.1  $[\text{M} + \text{H}]^+$ .

**4-Chloro-3-(3-(4-chloro-3-methylphenoxy)propyl)-1H-indole-2-carboxylic Acid (49)**. Coupling of ethyl 4-chloro-3-(3-hydroxypropyl)-1H-indole-2-carboxylate<sup>37</sup> and 4-chloro-3-methylphenol yielded **49**.  $^1\text{H}$  NMR (400 MHz, DMSO- $d_6$ ):  $\delta$  (ppm) 11.68 (s, 1H), 7.66 (d,  $J$  = 8.4 Hz, 1H), 7.26 (d,  $J$  = 8.4 Hz, 1H), 7.19 (t,  $J$  = 8.0 Hz, 1H), 7.07 (d,  $J$  = 7.6 Hz, 1H), 6.88–6.94 (m, 1H), 6.69–6.78 (m, 1H), 4.03 (t,  $J$  = 6.4 Hz, 2H), 3.45 (t,  $J$  = 7.2 Hz, 2H), 2.27 (s, 3H), 2.01–2.08 (m, 2H); >98% at 215 nm, MS (ESI)  $m/z$  = 378.1  $[\text{M} + \text{H}]^+$ .

**4-Chloro-3-(3-(4-chloro-3,5-dimethylphenoxy)propyl)-1H-indole-2-carboxylic Acid (50)**. Coupling of ethyl 4-chloro-3-(3-hydroxypropyl)-1H-indole-2-carboxylate<sup>37</sup> and 4-chloro-3,5-dimethylphenol yielded **50**.  $^1\text{H}$  NMR (400 MHz, DMSO- $d_6$ ):  $\delta$  (ppm) 11.70 (s, 1H), 7.67 (d,  $J$  = 8.4 Hz, 1H), 7.19 (t,  $J$  = 7.6 Hz, 1H), 7.07 (d,  $J$  = 7.6 Hz, 1H), 6.69 (s, 2H), 4.20 (t,  $J$  = 6.4 Hz, 2H), 3.44 (t,  $J$  = 7.2 Hz, 2H), 2.28 (s, 6H), 1.97–2.08 (m, 2H); >98% at 215 nm, MS (ESI)  $m/z$  = 392.1  $[\text{M} + \text{H}]^+$ .

**4-Chloro-3-(3-(naphthalen-1-yloxy)propyl)-1H-indole-2-carboxylic Acid (51)**. Coupling of ethyl 4-chloro-3-(3-hydroxypropyl)-1H-indole-2-carboxylate<sup>37</sup> and 1-naphthol yielded **51**.  $^1\text{H}$  NMR (400 MHz, DMSO- $d_6$ ):  $\delta$  (ppm) 11.68 (s, 1H), 8.18 (d,  $J$  = 8.0 Hz, 1H), 7.86 (d,  $J$  = 7.6 Hz, 1H), 7.35–7.57 (m, 5H), 7.21 (d,  $J$  = 8.0 Hz, 1H), 7.09 (d,  $J$  = 7.2 Hz, 1H), 6.94 (d,  $J$  = 7.2 Hz, 1H), 6.69–6.78 (m,  $J$  = 7.2 Hz, 1H), 4.25 (t,  $J$  = 6.0 Hz, 2H), 3.60 (t,  $J$  = 7.6 Hz, 2H), 2.16–2.25 (m, 2H); >98% at 215 nm, MS (ESI)  $m/z$  = 380.1  $[\text{M} + \text{H}]^+$ .

**6-Chloro-3-(3-(4-chloro-3-methylphenoxy)propyl)-1H-indole-2-carboxylic Acid (52)**. Coupling of ethyl 6-chloro-3-(3-hydroxypropyl)-1H-indole-2-carboxylate<sup>37</sup> and 4-chloro-3-methylphenol yielded **52**.  $^1\text{H}$  NMR (400 MHz, DMSO- $d_6$ ):  $\delta$  (ppm) 11.64 (s, 1H), 7.66 (d,  $J$  = 8.8 Hz, 1H), 7.40 (s, 1H), 7.26 (d,  $J$  = 8.8 Hz, 1H), 7.02 (d,  $J$  = 6.8 Hz, 1H), 7.07 (d,  $J$  = 7.6 Hz, 1H), 6.89 (s, 1H), 6.80 (d,  $J$  = 6.0 Hz, 1H), 3.93 (t,  $J$  = 6.4 Hz, 2H), 3.17 (t,  $J$  = 7.2 Hz, 2H), 2.27 (s, 3H), 1.95–2.08 (m, 2H); >98% at 215 nm, MS (ESI)  $m/z$  = 378.1  $[\text{M} + \text{H}]^+$ .

**6-Chloro-3-(3-(4-chloro-3,5-dimethylphenoxy)propyl)-1H-indole-2-carboxylic Acid (53)**. Coupling of ethyl 6-chloro-3-(3-hydroxypropyl)-1H-indole-2-carboxylate<sup>37</sup> and 4-chloro-3,5-dimethylphenol yielded **53**.  $^1\text{H}$  NMR (400 MHz, DMSO- $d_6$ ):  $\delta$  (ppm) 11.60 (s, 1H), 7.66 (d,  $J$  = 8.4 Hz, 1H), 7.40 (s, 1H), 7.02 (d,  $J$  = 7.2 Hz, 1H), 6.73 (s, 2H), 3.92 (t,  $J$  = 6.4 Hz, 2H), 3.17 (t,  $J$  = 7.6 Hz, 2H), 2.27 (s, 6H), 1.95–2.05 (m, 2H); >98% at 215 nm, MS (ESI)  $m/z$  = 392.1  $[\text{M} + \text{H}]^+$ .

**6-Chloro-3-(3-(naphthalen-1-yloxy)propyl)-1H-indole-2-carboxylic Acid (54)**. Coupling of ethyl 6-chloro-3-(3-hydroxypropyl)-1H-indole-2-carboxylate<sup>37</sup> and 1-naphthol yielded **54**.  $^1\text{H}$  NMR (400 MHz, DMSO- $d_6$ ):  $\delta$  (ppm) 11.62 (s, 1H), 8.19 (d,  $J$  = 7.6 Hz, 1H), 7.86 (d,  $J$  = 7.6 Hz, 1H), 7.69 (d,  $J$  = 8.4 Hz, 1H), 7.33–7.57 (m, 5H), 6.97 (d,  $J$  = 8.0 Hz, 1H), 6.87 (d,  $J$  = 8.0 Hz, 1H), 4.15 (t,  $J$  = 6.4 Hz, 2H), 3.27–3.37 (m, 2H), 2.16–2.25 (m, 2H); >98% at 215 nm, MS (ESI)  $m/z$  = 380.1  $[\text{M} + \text{H}]^+$ .

**6-Chloro-3-(3-((5,6,7,8-tetrahydronaphthalen-1-yl)oxy)propyl)-1H-indole-2-carboxylic Acid (55)**. Coupling of ethyl 6-chloro-3-(3-hydroxypropyl)-1H-indole-2-carboxylate<sup>37</sup> and 5,6,7,8-tetrahydronaphthalen-1-ol yielded **55**; >98% at 215 nm, MS (ESI)  $m/z$  = 384.1  $[\text{M} + \text{H}]^+$ .

**3-(3-(4-Chloro-3,5-dimethylphenoxy)propyl)-1-methyl-1H-indole-2-carboxylic Acid (56)**. General Procedure for Alkylation of Indole NH. To a solution of ethyl 3-(3-(4-chloro-3,5-dimethylphenoxy)propyl)-1H-indole-2-carboxylate (15 mg, 0.04

mmol) in DMF (0.8 mL) was added NaH (3.0 mg, 0.075 mmol, 60% in mineral oil) at 20 °C under Ar. The reaction mixture was stirred for 20 min at 20 °C. Then MeI (34 mg, 0.24 mmol) was added. The reaction mixture was stirred for an additional 1 h and then quenched by addition of water. The reaction mixture was extracted with  $\text{CH}_2\text{Cl}_2$ . Combined organic layer was concentrated in vacuo, and the residue was purified by reverse phase preparative HPLC to give the product as a solid (12 mg, 0.03 mmol): >98% at 215 nm, MS (ESI)  $m/z$  = 400.2  $[\text{M} + \text{H}]^+$ .

The title compound was obtained by following the general procedure for saponification outlined above as a white solid.  $^1\text{H}$  NMR (400 MHz, DMSO- $d_6$ ):  $\delta$  (ppm) 7.67 (d,  $J$  = 8.0 Hz, 1H), 7.52 (d,  $J$  = 8.0 Hz, 1H), 7.32 (t,  $J$  = 7.2 Hz, 1H), 7.07 (t,  $J$  = 7.2 Hz, 1H), 6.75 (s, 2H), 3.91–3.99 (m, 5H), 3.18 (t,  $J$  = 7.2 Hz, 2H), 2.23 (s, 6H), 1.96–2.05 (m, 2H); >98% at 215 nm, MS (ESI)  $m/z$  = 372.1  $[\text{M} + \text{H}]^+$ .

Compounds **57–59** were prepared following the general procedure outlined above in library format. Purity of all final compounds was determined by HPLC analysis and is >95%. All compounds were isolated as solids.

**1-Methyl-3-(3-(naphthalen-1-yloxy)propyl)-1H-indole-2-carboxylic Acid (57)**. Methylation of ethyl 3-(3-(naphthalen-1-yloxy)propyl)-1H-indole-2-carboxylate by MeI yielded **57**.  $^1\text{H}$  NMR (400 MHz, DMSO- $d_6$ ):  $\delta$  (ppm) 8.22 (d,  $J$  = 6.4 Hz, 1H), 7.87 (d,  $J$  = 6.4 Hz, 1H), 7.70 (d,  $J$  = 8.0 Hz, 1H), 7.36–7.58 (m, 5H), 7.30 (t,  $J$  = 7.6 Hz, 1H), 7.06 (t,  $J$  = 7.6 Hz, 1H), 6.87 (d,  $J$  = 7.6 Hz, 1H), 4.16 (t,  $J$  = 6.0 Hz, 2H), 3.97 (s, 3H), 3.30–3.40 (m, 2H), 2.15–2.25 (m, 2H); >98% at 215 nm, MS (ESI)  $m/z$  = 360.1  $[\text{M} + \text{H}]^+$ .

**6-Chloro-3-(3-(4-chloro-3,5-dimethylphenoxy)propyl)-1-methyl-1H-indole-2-carboxylic Acid (58)**. Methylation of ethyl 6-chloro-3-(3-(4-chloro-3,5-dimethylphenoxy)propyl)-1H-indole-2-carboxylate by MeI yielded **58**.  $^1\text{H}$  NMR (400 MHz, DMSO- $d_6$ ):  $\delta$  (ppm) 7.79–7.57 (m, 2H), 7.07 (dd,  $J$  = 8.6, 1.7 Hz, 1H), 6.73 (s, 2H), 3.97–3.89 (m, 5H), 3.20–3.10 (m, 2H), 2.27 (s, 6H), 2.06–1.93 (m, 2H); >98% at 215 nm, MS (ESI) 1.83 min,  $m/z$  = 428  $[\text{M} + \text{Na}]^+$ .

**1-Benzyl-3-(3-(naphthalen-1-yloxy)propyl)-1H-indole-2-carboxylic Acid (59)**. Benzylation of ethyl 3-(3-(naphthalen-1-yloxy)propyl)-1H-indole-2-carboxylate by benzyl bromide yielded **59**.  $^1\text{H}$  NMR (400 MHz, DMSO- $d_6$ ):  $\delta$  (ppm) 8.18–8.24 (m, 1H), 7.87 (d,  $J$  = 7.2 Hz, 1H), 7.72–7.80 (m, 1H), 7.42–7.56 (m, 3H), 7.35–7.40 (m, 1H), 7.15–7.30 (m, 5H), 6.95–7.10 (m, 3H), 6.83–6.90 (m, 1H), 5.84 (s, 2H), 4.17 (t,  $J$  = 6.0 Hz, 2H), 3.30–3.40 (m, 2H), 2.15–2.25 (m, 2H); >98% at 215 nm, MS (ESI)  $m/z$  = 436.2  $[\text{M} + \text{H}]^+$ .

**1-(3-(4-Chloro-3-methylphenoxy)propyl)-1H-indole-2-carboxylic Acid (69)**. The title compound was obtained by following the general procedure for phenol analogue coupling and saponification outlined above using ethyl 1-(3-hydroxypropyl)-1H-indole-2-carboxylate and 4-chloro-3-methylphenol as a white solid: >98% at 215 nm, MS (ESI)  $m/z$  = 344.1  $[\text{M} + \text{H}]^+$ .

**1-(3-(4-Chloro-3,5-dimethylphenoxy)propyl)-1H-indole-2-carboxylic Acid (70)**. The title compound was obtained by following the general procedure for phenol analogue coupling and saponification outlined above using ethyl 1-(3-hydroxypropyl)-1H-indole-2-carboxylate and 4-chloro-3,5-dimethylphenol as a white solid: >98% at 215 nm, MS (ESI)  $m/z$  = 357.1  $[\text{M} + \text{H}]^+$ .

**1-(3-(Naphthalen-1-yloxy)propyl)-1H-indole-2-carboxylic Acid (71)**. The title compound was obtained by following the general procedure for phenol analogue coupling and saponification outlined above using ethyl 1-(3-hydroxypropyl)-1H-indole-2-carboxylate and 1-naphthol as a white solid.  $^1\text{H}$  NMR (400 MHz, DMSO- $d_6$ ):  $\delta$  (ppm) 8.26 (d,  $J$  = 7.2 Hz, 1H), 7.87 (d,  $J$  = 7.2 Hz, 1H), 7.69 (d,  $J$  = 8.0 Hz, 1H), 7.37–7.57 (m, 4H), 7.35 (t,  $J$  = 8.0 Hz, 1H), 7.15–7.25 (m, 2H), 7.07 (t,  $J$  = 7.2 Hz, 1H), 6.85 (d,  $J$  = 7.2 Hz, 1H), 4.89 (t,  $J$  = 6.8 Hz, 2H), 4.23 (t,  $J$  = 7.2 Hz, 2H), 2.15–2.25 (m, 2H); >98% at 215 nm, MS (ESI)  $m/z$  = 346.1  $[\text{M} + \text{H}]^+$ .

**1-(3-(Naphthalen-1-yloxy)propyl)-1H-indole-2-carboxamide (72)**. To a solution of 1-(3-(naphthalen-1-yloxy)propyl)-1H-indole-2-carboxylic acid (15 mg, 0.043 mmol) in  $\text{CH}_2\text{Cl}_2$  (1.0 mL) was added oxalyl chloride (37  $\mu\text{L}$ , 0.43 mmol) followed by a drops of  $N,N$ -dimethylformamide at room temperature under Ar. The reaction mixture was stirred for 3 h at room temperature and then concentrated under vacuum. The residue was redissolved in  $\text{CH}_2\text{Cl}_2$  (0.5 mL), and

concentrated  $\text{NH}_4\text{OH}$  aqueous solution (0.67 mL) was added. The reaction mixture was stirred for 2 h and then extracted with ethyl acetate. The organic layer was concentrated in vacuo, and the residue was purified by reverse phase preparative HPLC to give the product as a white solid (11 mg, 0.032 mmol).  $^1\text{H}$  NMR (400 MHz,  $\text{DMSO}-d_6$ ):  $\delta$  (ppm) 8.24–8.30 (m, 1H), 7.99 (br, 2H), 7.82–7.90 (m, 1H), 7.63 (d,  $J$  = 8.0, 1H), 7.47–7.60 (m, 3H), 7.42–7.46 (m, 1H), 7.35–7.40 (m, 1H), 7.19 (s, 1H), 7.14 (t,  $J$  = 7.2 Hz, 1H), 7.06 (t,  $J$  = 7.2 Hz, 1H), 6.84 (t,  $J$  = 7.2 Hz, 1H), 4.86 (t,  $J$  = 7.2 Hz, 2H), 4.12 (t,  $J$  = 6.0 Hz, 2H), 2.25–2.35 (m, 2H); >98% at 215 nm, MS (ESI)  $m/z$  = 345.1  $[\text{M} + \text{H}]^+$ .

## ■ ASSOCIATED CONTENT

### ■ Supporting Information

Mcl-1 protein sequence used for X-ray crystallography,  $^1\text{H}$ – $^{15}\text{N}$  HMQC spectra of Mcl-1 with and without compound **53**, FPA dose–response curve of compound **53** displacing a FITC-labeled BAK peptide from Mcl-1, and synthesis of intermediates. This material is available free of charge via the Internet at <http://pubs.acs.org>.

### Accession Codes

Atom coordinates and structure factors for Mcl-1/ligand complexes have been deposited at the Protein Data Bank (4HW2, 4HW3, and 4HW4).

## ■ AUTHOR INFORMATION

### Corresponding Author

\*Phone: +1 (615) 322 6303. Fax: +1 (615) 875 3236. E-mail: [stephen.fesik@vanderbilt.edu](mailto:stephen.fesik@vanderbilt.edu).

### Notes

The authors declare no competing financial interest.

## ■ ACKNOWLEDGMENTS

The authors thank co-workers at the High-Throughput Screening Core facility of Vanderbilt University, TN, for compound management and providing the instrumentation to perform the binding assay and Dr. Olivia Rossanese for critical reading of the manuscript. The pDEST-HisMBP entry plasmid and a TEV protease expression vector were kindly provided by Dr. David S. Waugh (National Cancer Institute) and Dr. Arie Geerloff (Helmholz Zentrum München, Germany), respectively. This research was supported by the U.S. National Institutes of Health, NIH Director's Pioneer Award DP1OD006933/DP1CA174419 to S.W.F., an ARRA stimulus Grant RC2A148375 to L. J. Marnett, and a career development award to S.W.F. from a NCI SPORE grant in breast cancer (Grant P50CA098131) to C. L. Arteaga. This work was also funded by the American Cancer Society (Postdoctoral Fellowship, Grant PF1110501CDD) to J.P.B. The Biomolecular NMR Facility at Vanderbilt University is supported in part by a NIH SIG Grant 1S-10RR025677-01 and Vanderbilt University matching funds. Use of the Advanced Photon Source was supported by the U.S. Department of Energy, Office of Science, Office of Basic Energy Sciences, under Contract No. DE-AC02-06CH11357. Use of the LS-CAT Sector 21 was supported by the Michigan Economic Development Corporation and the Michigan Technology Tri-Corridor for the support of this research program (Grant 08SP1000817).

## ■ ABBREVIATIONS USED

FBDD, fragment-based drug discovery; Mcl-1, myeloid cell leukemia 1; Bcl-2, B-cell lymphoma 2; Bcl-xL, B-cell lymphoma extra large; BH3, Bcl-2 homology domain 3; CSP, chemical shift perturbation; FITC, fluorescein isothiocyanate; FPA, fluorescence polarization anisotropy

## ■ REFERENCES

- (1) Danial, N. N.; Korsmeyer, S. J. Cell death: critical control points. *Cell* **2004**, *116*, 205–219.
- (2) Adams, J. M.; Cory, S. The Bcl-2 apoptotic switch in cancer development and therapy. *Oncogene* **2007**, *26*, 1324–1337.
- (3) Willis, S. N.; Fletcher, J. I.; Kaufmann, T.; van Delft, M. F.; Chen, L.; Czabotar, P. E.; Ierino, H.; Lee, E. F.; Fairlie, W. D.; Bouillet, P.; Strasser, A.; Kluck, R. M.; Adams, J. M.; Huang, D. C. S. Apoptosis initiated when BH3 ligands engage multiple Bcl-2 homologs, not Bax or Bak. *Science* **2007**, *315*, 856–859.
- (4) Beroukhi, R.; Mermel, C. H.; Porter, D.; Wei, G.; Raychaudhuri, S.; Donovan, J.; Barretina, J.; Boehm, J. S.; Dobson, J.; Urashima, M.; McHenry, K. T.; Pinchback, R. M.; Ligon, A. H.; Cho, Y.-J.; Haery, L.; Greulich, H.; Reich, M.; Winckler, W.; Lawrence, M. S.; Weir, B. A.; Tanaka, K. E.; Chiang, D. Y.; Bass, A. J.; Loo, A.; Hoffman, C.; Prensner, J.; Liefeld, T.; Gao, Q.; Yecies, D.; Signoretti, S.; Maher, E.; Kaye, F. J.; Sasaki, H.; Tepper, J. E.; Fletcher, J. A.; Tabernero, J.; Baselga, J.; Tsao, M.-S.; Demicheli, F.; Rubin, M. A.; Janne, P. A.; Daly, M. J.; Nucera, C.; Levine, R. L.; Ebert, B. L.; Gabriel, S.; Rustgi, A. K.; Antonescu, C. R.; Ladanyi, M.; Letai, A.; Garraway, L. A.; Loda, M.; Beer, D. G.; True, L. D.; Okamoto, A.; Pomeroy, S. L.; Singer, S.; Golub, T. R.; Lander, E. S.; Getz, G.; Sellers, W. R.; Meyerson, M. The landscape of somatic copy-number alteration across human cancers. *Nature* **2010**, *463*, 899–905.
- (5) Wei, G.; Margolin, A. A.; Haery, L.; Brown, E.; Cucolo, L.; Julian, B.; Shehata, S.; Kung, A. L.; Beroukhi, R.; Golub, T. R. Chemical genomics identifies small-molecule MCL1 repressors and BCL-XL as a predictor of MCL1 dependency. *Cancer Cell* **2012**, *21*, 547–562.
- (6) Song, L.; Coppola, D.; Livingston, S.; Cress, D.; Haura, E. B. Mcl-1 regulates survival and sensitivity to diverse apoptotic stimuli in human non-small cell lung cancer cells. *Cancer Biol. Ther.* **2005**, *4*, 267–276.
- (7) Ding, Q.; He, X.; Xia, W.; Hsu, J.-M.; Chen, C.-T.; Li, L.-Y.; Lee, D.-F.; Yang, J.-Y.; Xie, X.; Liu, J.-C.; Hung, M.-C. Myeloid cell leukemia-1 inversely correlates with glycogen synthase kinase-3 $\beta$  activity and associates with poor prognosis in human breast cancer. *Cancer Res.* **2007**, *67*, 4564–4571.
- (8) Krajewska, M.; Krajewski, S.; Epstein, J. I.; Shabai, A.; Sauvageot, J.; Song, K.; Kitada, S.; Reed, J. C. Immunohistochemical analysis of bcl-2, bax, bcl-X, and mcl-1 expression in prostate cancers. *Am. J. Pathol.* **1996**, *148*, 1567–1576.
- (9) Miyamoto, Y.; Hosotani, R.; Wada, M.; Lee, J. U.; Koshiba, T.; Fujimoto, K.; Tsuji, S.; Nakajima, S.; Doi, R.; Kato, M.; Shimada, Y.; Imamura, M. Immunohistochemical analysis of Bcl-2, Bax, Bcl-X, and Mcl-1 expression in pancreatic cancers. *Oncology* **1999**, *56*, 73–82.
- (10) Brotin, E.; Meryet-Figuière, M.; Simonin, K.; Duval, R. E.; Villedieu, M.; Leroy-Dudal, J.; Saison-Beahmoaras, E.; Gauduchon, P.; Denoyelle, C.; Poulain, L. Bcl-XL and MCL-1 constitute pertinent targets in ovarian carcinoma and their concomitant inhibition is sufficient to induce apoptosis. *Int. J. Cancer* **2010**, *126*, 885–895.
- (11) Derenne, S.; Monia, B.; Dean, N. M.; Taylor, J. K.; Rapp, M.-J.; Harousseau, J.-L.; Bataille, R.; Amiot, M. Antisense strategy shows that Mcl-1 rather than Bcl-2 or Bcl-x(L) is an essential survival protein of human myeloma cells. *Blood* **2002**, *100*, 194–199.
- (12) Andersen, M. H.; Becker, J. C.; Thor Straten, P. The antiapoptotic member of the Bcl-2 family Mcl-1 is a CTL target in cancer patients. *Leukemia* **2005**, *19*, 484–485.
- (13) Kang, M. H.; Wan, Z.; Kang, Y. H.; Spoto, R.; Reynolds, C. P. Mechanism of synergy of N-(4-hydroxyphenyl)retinamide and ABT-737 in acute lymphoblastic leukemia cell lines: Mcl-1 inactivation. *J. Natl. Cancer Inst.* **2008**, *100*, 580–595.
- (14) Wertz, I. E.; Kusam, S.; Lam, C.; Okamoto, T.; Sandoval, W.; Anderson, D. J.; Helgason, E.; Ernst, J. A.; Eby, M.; Liu, J.; Belmont, L. D.; Kaminker, J. S.; O'Rourke, K. M.; Pujara, K.; Kohli, P. B.; Johnson, A. R.; Chiu, M. L.; Lill, J. R.; Jackson, P. K.; Fairbrother, W. J.; Seshagiri, S.; Ludlam, M. J. C.; Leong, K. G.; Dueber, E. C.; Maecker, H.; Huang, D. C. S.; Dixit, V. M. Sensitivity to antitubulin chemotherapeutics is regulated by MCL1 and FBW7. *Nature* **2011**, *471*, 110–114.
- (15) Wei, S.-H.; Dong, K.; Lin, F.; Wang, X.; Li, B.; Shen, J.-J.; Zhang, Q.; Wang, R.; Zhang, H.-Z. Inducing apoptosis and enhancing chemosensitivity to gemcitabine via RNA interference targeting Mcl-1



gene in pancreatic carcinoma cell. *Cancer Chemother. Pharmacol.* **2008**, *62*, 1055–1064.

(16) van Delft, M. F.; Wei, A. H.; Mason, K. D.; Vandenberg, C. J.; Chen, L.; Czabotar, P. E.; Willis, S. N.; Scott, C. L.; Day, C. L.; Cory, S.; Adams, J. M.; Roberts, A. W.; Huang, D. C. S. The BH3 mimetic ABT-737 targets selective Bcl-2 proteins and efficiently induces apoptosis via Bak/Bax if Mcl-1 is neutralized. *Cancer Cell* **2006**, *10*, 389–399.

(17) Varin, E.; Denoyelle, C.; Brodin, E.; Meryet-Figuière, M.; Giffard, F.; Abeillard, E.; Goux, D.; Gauduchon, P.; Icard, P.; Poulain, L. Downregulation of Bcl-xL and Mcl-1 is sufficient to induce cell death in mesothelioma cells highly refractory to conventional chemotherapy. *Carcinogenesis* **2010**, *31*, 984–993.

(18) Olberding, K. E.; Wang, X.; Zhu, Y.; Pan, J.; Rai, S. N.; Li, C. Actinomycin D synergistically enhances the efficacy of the BH3 mimetic ABT-737 by downregulating Mcl-1 expression. *Cancer Biol. Ther.* **2010**, *10*, 918–929.

(19) Zhang, H.; Guttikonda, S.; Roberts, L.; Uziel, T.; Semizarov, D.; Elmore, S. W.; Levenson, J. D.; Lam, L. T. Mcl-1 is critical for survival in a subgroup of non-small-cell lung cancer cell lines. *Oncogene* **2011**, *30*, 1963–1968.

(20) Rega, M. F.; Wu, B.; Wei, J.; Zhang, Z.; Cellitti, J. F.; Pellecchia, M. SAR by interligand nuclear Overhauser effects (ILOEs) based discovery of acylsulfonamide compounds active against Bcl-x(L) and Mcl-1. *J. Med. Chem.* **2011**, *54*, 6000–6013.

(21) Cohen, N. A.; Stewart, M. L.; Gavathiotis, E.; Tepper, J. L.; Bruekner, S. R.; Koss, B.; Opferman, J. T.; Walensky, L. D. A competitive stapled peptide screen identifies a selective small molecule that overcomes MCL-1-dependent leukemia cell survival. *Chem. Biol.* **2012**, *19*, 1175–1186.

(22) Kim, Y. B.; Balasis, M. E.; Doi, K.; Berndt, N.; Duboulay, C.; Hu, C.-C. A.; Guida, W.; Wang, H.-G.; Sebt, S. M.; Del Valle, J. R. Synthesis and evaluation of substituted hexahydronaphthalenes as novel inhibitors of the Mcl-1/BimBH3 interaction. *Bioorg. Med. Chem. Lett.* **2012**, *22*, 5961–5965.

(23) Stewart, M. L.; Fire, E.; Keating, A. E.; Walensky, L. D. The MCL-1 BH3 helix is an exclusive MCL-1 inhibitor and apoptosis sensitizer. *Nat. Chem. Biol.* **2010**, *6*, 595–601.

(24) Muppidi, A.; Doi, K.; Edwardraja, S.; Drake, E. J.; Gulick, A. M.; Wang, H.-G.; Lin, Q. Rational design of proteolytically stable, cell-permeable peptide-based selective Mcl-1 inhibitors. *J. Am. Chem. Soc.* **2012**, *134*, 14734–14737.

(25) Shuker, S. B.; Hajduk, P. J.; Meadows, R. P.; Fesik, S. W. Discovering high-affinity ligands for proteins: SAR by NMR. *Science* **1996**, *274*, 1531–1534.

(26) Murray, C. W.; Blundell, T. L. Structural biology in fragment-based drug design. *Curr. Opin. Struct. Biol.* **2010**, *20*, 497–507.

(27) Oltsersdorf, T.; Elmore, S. W.; Shoemaker, A. R.; Armstrong, R. C.; Augeri, D. J.; Belli, B. A.; Bruncko, M.; Deckwerth, T. L.; Dinges, J.; Hajduk, P. J.; Joseph, M. K.; Kitada, S.; Korsmeyer, S. J.; Kunzer, A. R.; Letai, A.; Li, C.; Mitten, M. J.; Nettesheim, D. G.; Ng, S.; Nimmer, P. M.; O'Connor, J. M.; Oleksijew, A.; Petros, A. M.; Reed, J. C.; Shen, W.; Tahir, S. K.; Thompson, C. B.; Tomaselli, K. J.; Wang, B.; Wendt, M. D.; Zhang, H.; Fesik, S. W.; Rosenberg, S. H. An inhibitor of Bcl-2 family proteins induces regression of solid tumours. *Nature* **2005**, *435*, 677–681.

(28) Tse, C.; Shoemaker, A. R.; Adickes, J.; Anderson, M. G.; Chen, J.; Jin, S.; Johnson, E. F.; Marsh, K. C.; Mitten, M. J.; Nimmer, P.; Roberts, L.; Tahir, S. K.; Xiao, Y.; Yang, X.; Zhang, H.; Fesik, S.; Rosenberg, S. H.; Elmore, S. W. ABT-263: a potent and orally bioavailable Bcl-2 family inhibitor. *Cancer Res.* **2008**, *68*, 3421–3428.

(29) Huth, J. R.; Park, C.; Petros, A. M.; Kunzer, A. R.; Wendt, M. D.; Wang, X.; Lynch, C. L.; Mack, J. C.; Swift, K. M.; Judge, R. A.; Chen, J.; Richardson, P. L.; Jin, S.; Tahir, S. K.; Matayoshi, E. D.; Dorwin, S. A.; Lador, U. S.; Severin, J. M.; Walter, K. A.; Bartley, D. M.; Fesik, S. W.; Elmore, S. W.; Hajduk, P. J. Discovery and design of novel HSP90 inhibitors using multiple fragment-based design strategies. *Chem. Biol. Drug Des.* **2007**, *70*, 1–12.

(30) Wyss, D. F.; Wang, Y.-S.; Eaton, H. L.; Strickland, C.; Voigt, J. H.; Zhu, Z.; Stamford, A. W. Combining NMR and X-ray crystallography in

fragment-based drug discovery: discovery of highly potent and selective BACE-1 inhibitors. *Top. Curr. Chem.* **2012**, *317*, 83–114.

(31) Kuntz, I. D.; Chen, K.; Sharp, K. A.; Kollman, P. A. The maximal affinity of ligands. *Proc. Natl. Acad. Sci. U.S.A.* **1999**, *96*, 9997–10002.

(32) Murray, C. W.; Rees, D. C. The rise of fragment-based drug discovery. *Nat. Chem.* **2009**, *1*, 187–192.

(33) Bruncko, M.; Song, X.; Ding, H.; Tao, Z.-F.; Kunzer, A. R. 7-Nonsubstituted Indoles as Mcl-1 Inhibitors and Their Preparation. PCT Int. Appl. WO-0130970-A1, 2008.

(34) Elmore, S. W.; Souers, A. J.; Bruncko, M.; Song, X.; Wang, X.; Hasvold, L. A.; Wang, L.; Kunzer, A. R.; Park, C.-M.; Wendt, M. D.; Tao, Z.-F. 7-Substituted Indoles as Mcl-1 Protein Inhibitors and Their Preparation. PCT Int. Appl. WO-0131000-A2, 2008.

(35) Fire, E.; Gullá, S. V.; Grant, R. A.; Keating, A. E. Mcl-1-Bim complexes accommodate surprising point mutations via minor structural changes. *Protein Sci.* **2010**, *19*, S07–S19.

(36) Petros, A. M.; Olejniczak, E. T.; Fesik, S. W. Structural biology of the Bcl-2 family of proteins. *Biochim. Biophys. Acta* **2004**, *1644*, 83–94.

(37) Salituro, F. G.; Harrison, B. L.; Baron, B. M.; Nyce, P. L.; Stewart, K. T.; McDonald, I. A. 3-(2-Carboxyindol-3-yl)propionic acid derivatives: antagonists of the strychnine-insensitive glycine receptor associated with the N-methyl-D-aspartate receptor complex. *J. Med. Chem.* **1990**, *33*, 2944–2946.

(38) Konopleva, M.; Contractor, R.; Tsao, T.; Samudio, I.; Ruvolo, P. P.; Kitada, S.; Deng, X.; Zhai, D.; Shi, Y.-X.; Sneed, T.; Verhaegen, M.; Soengas, M.; Ruvolo, V. R.; McQueen, T.; Schober, W. D.; Watt, J. C.; Jiffar, T.; Ling, X.; Marini, F. C.; Harris, D.; Dietrich, M.; Estrov, Z.; McCubrey, J.; May, W. S.; Reed, J. C.; Andreeff, M. Mechanisms of apoptosis sensitivity and resistance to the BH3 mimetic ABT-737 in acute myeloid leukemia. *Cancer Cell* **2006**, *10*, 375–388.

(39) Schanda, P.; Brutscher, B. Very fast two-dimensional NMR spectroscopy for real-time investigation of dynamic events in proteins on the time scale of seconds. *J. Am. Chem. Soc.* **2005**, *127*, 8014–8015.

(40) Congreve, M.; Carr, R.; Murray, C.; Jhoti, H. A “rule of three” for fragment-based lead discovery? *Drug Discovery Today* **2003**, *8*, 876–877.

(41) Sattler, M.; Schleucher, J.; Griesinger, C. Heteronuclear multidimensional NMR experiments for the structure determination of proteins in solution employing pulsed. *Prog. Nucl. Magn. Reson. Spectrosc.* **1999**, *34*, 93–158.

(42) Schwieters, C. D.; Kuszewski, J. J.; Tjandra, N.; Clore, G. M. The Xplor-NIH NMR molecular structure determination package. *J. Magn. Reson.* **2003**, *160*, 65–73.

(43) Otwinowski, Z.; Minor, W. Processing of X-ray Diffraction Data Collected in Oscillation Mode. In *Macromolecular Crystallography. Part A*; Carter, C. W., Jr., Sweet, R. M., Eds.; Academic Press: San Diego, CA, 1997; Vol. 276, pp 307–326.

(44) McCoy, A. J.; Grosse-Kunstleve, R. W.; Adams, P. D.; Winn, M. D.; Storoni, L. C.; Read, R. J. Phaser crystallographic software. *J. Appl. Crystallogr.* **2007**, *40*, 658–674.

(45) Winn, M. D.; Ballard, C. C.; Cowtan, K. D.; Dodson, E. J.; Emsley, P.; Evans, P. R.; Keegan, R. M.; Krissinel, E. B.; Leslie, A. G. W.; McCoy, A.; McNicholas, S. J.; Murshudov, G. N.; Pannu, N. S.; Potterton, E. A.; Powell, H. R.; Read, R. J.; Vagin, A.; Wilson, K. S. Overview of the CCP4 suite and current developments. *Acta Crystallogr., Sect. D: Biol. Crystallogr.* **2011**, *67*, 235–242.

(46) Adams, P. D.; Grosse-Kunstleve, R. W.; Hung, L. W.; Ioerger, T. R.; McCoy, A. J.; Moriarty, N. W.; Read, R. J.; Sacchettini, J. C.; Sauter, N. K.; Terwilliger, T. C. PHENIX: building new software for automated crystallographic structure determination. *Acta Crystallogr., Sect. D: Biol. Crystallogr.* **2002**, *58*, 1948–1954.

(47) Murshudov, G. N.; Skubák, P.; Lebedev, A. A.; Pannu, N. S.; Steiner, R. A.; Nicholls, R. A.; Winn, M. D.; Long, F.; Vagin, A. A. REFMACS for the refinement of macromolecular crystal structures. *Acta Crystallogr., Sect. D: Biol. Crystallogr.* **2011**, *67*, 355–367.

(48) Emsley, P.; Cowtan, K. Coot: model-building tools for molecular graphics. *Acta Crystallogr., Sect. D: Biol. Crystallogr.* **2004**, *60*, 2126–2132.

(49) *The PyMOL Molecular Graphics System*, version 1.5; Schrödinger, LLC: New York, 2010.

(50) Wang, Z. X.; Jiang, R. F. A novel two-site binding equation presented in terms of the total ligand concentration. *FEBS Lett.* **1996**, *392*, 245–249.

(51) Piemontese, L.; Carbonara, G.; Fracchiolla, G.; Laghezza, A.; Tortorella, P.; Loiodice, F. Convenient synthesis of some 3-phenyl-1-benzofuran-2-carboxylic acid derivatives as new potential inhibitors of CLC-Kb channels. *Heterocycles* **2010**, *81*, 2865–2872.

(52) Laskowski, R.; Macarthur, M.; Moss, D.; Thornton, J. PROCHECK: a program to check the stereochemical quality of protein structures. *J. Appl. Crystallogr.* **1993**, *26*, 283–291.